Trieste Observatory

Trieste 21.01.2015

Cosmic Reionization: Theoretical Modeling and Challenging Observations

Benedetta Ciardi

Max Planck Institute for Astrophysics

OUTLINE

- ✧ Available constraints on cosmic reionization
- ✧ Theoretical modeling
- ✧ 21cm observations
- ✧ What LOFAR can do
- ✧ Conclusions

Timeline in cosmic history

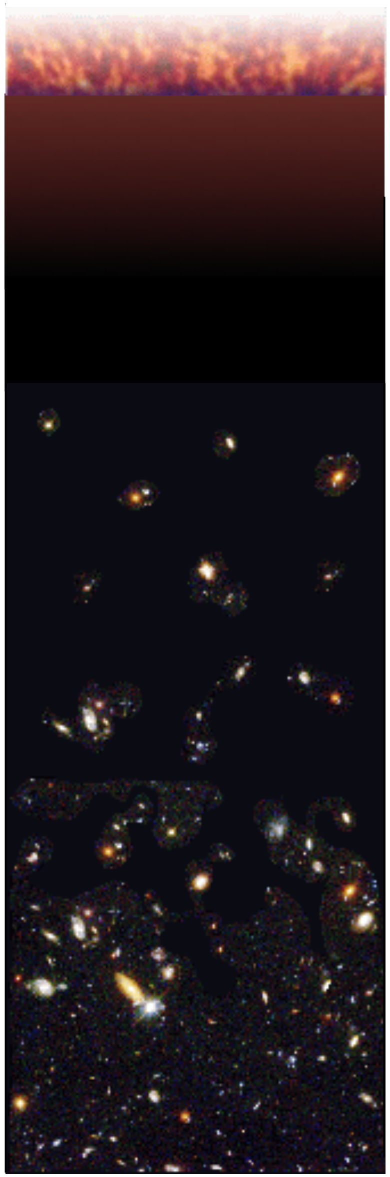

TIMELINE IN COSMIC HISTORY

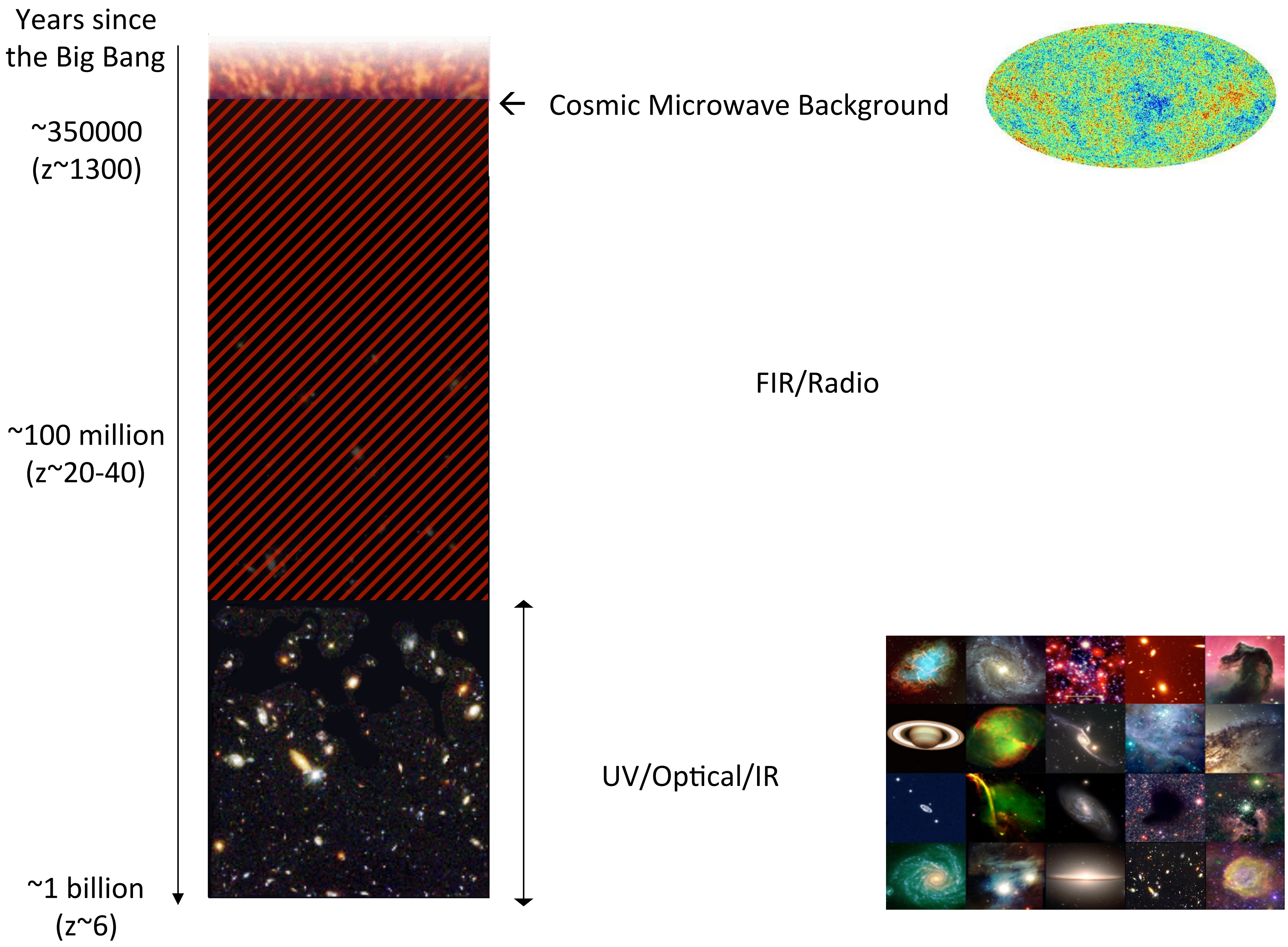

EVIDENCE FOR IGM REIONIZATION

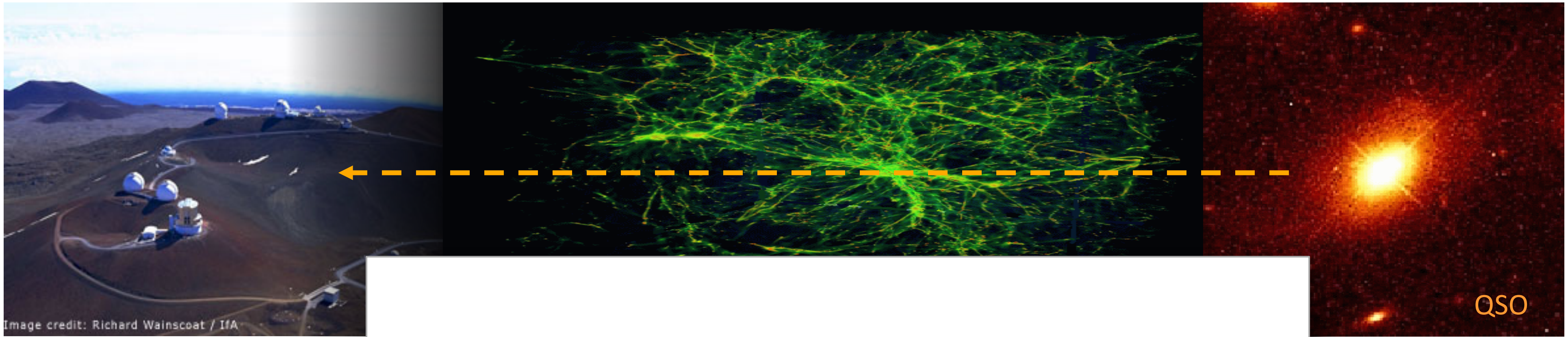

We observe Ly-alpha emission from high-z QSOs:

this indicates that the IGM is highly ionized

$$\tau_{HI} \approx 6.5 \cdot 10^5 x_{HI} \left(\frac{1+z}{10} \right)^{3/2}$$

$$x_{HI} = n_{HI} / n_H$$

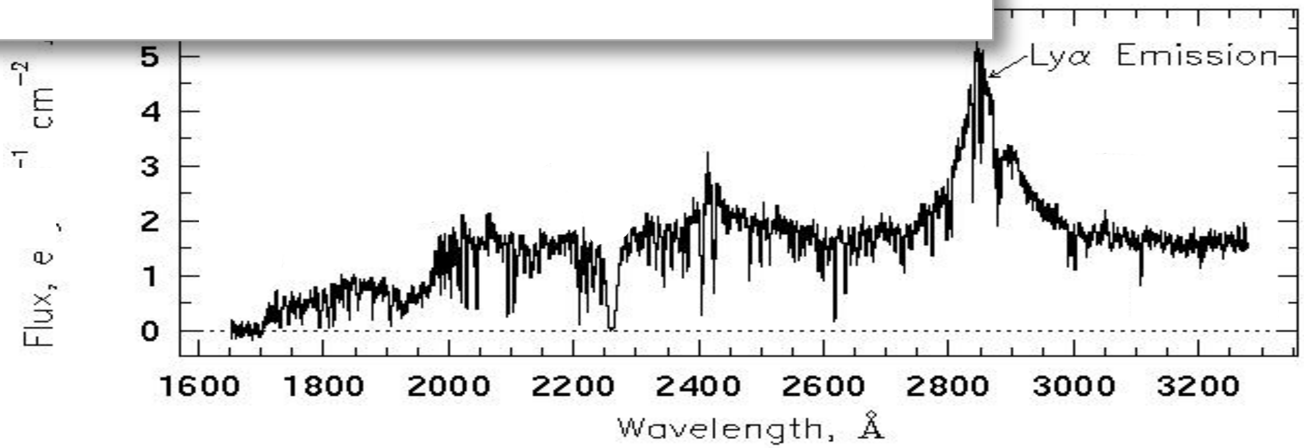

Constraints on the epoch of reionization

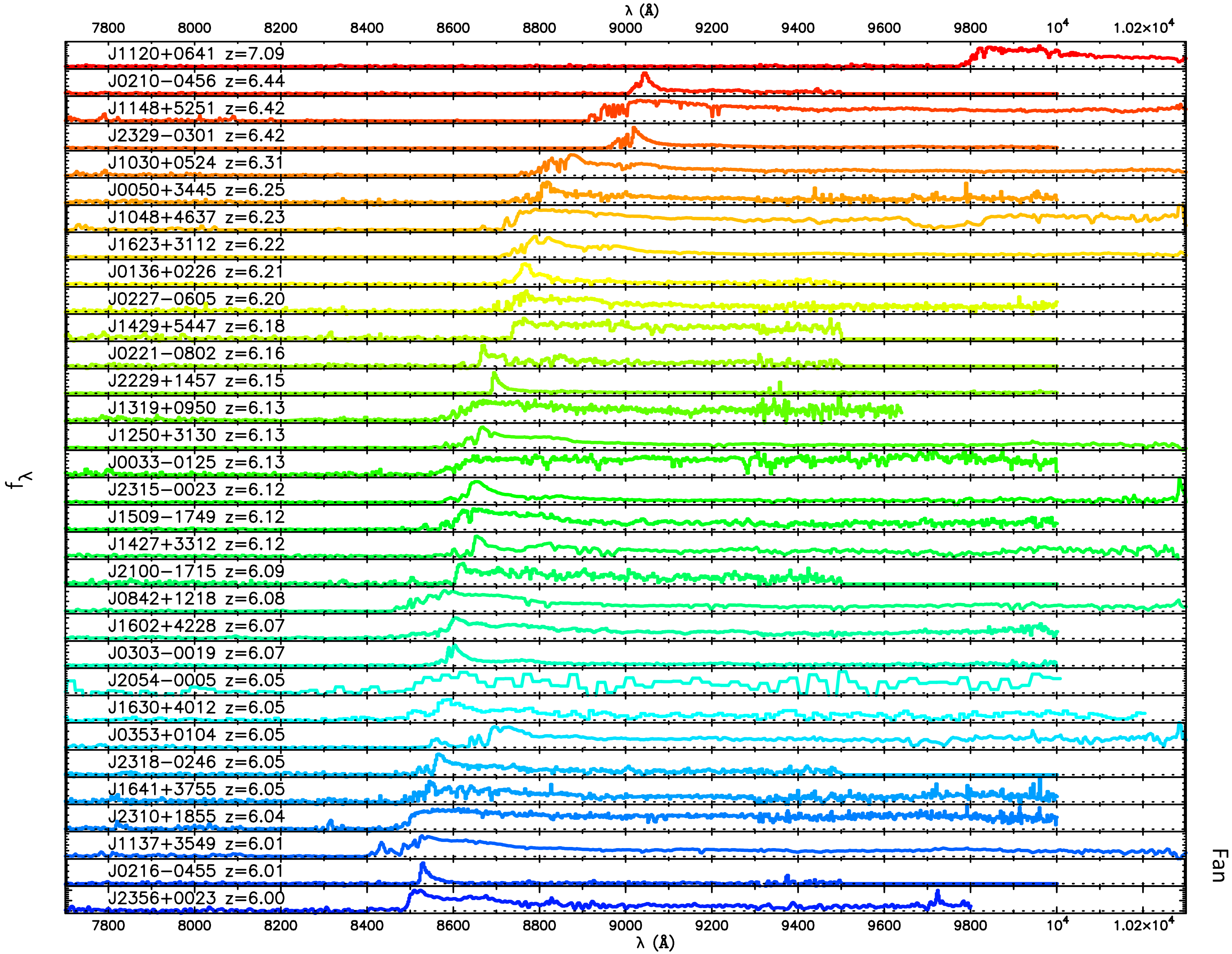

CONSTRAINTS ON THE EPOCH OF REIONIZATION

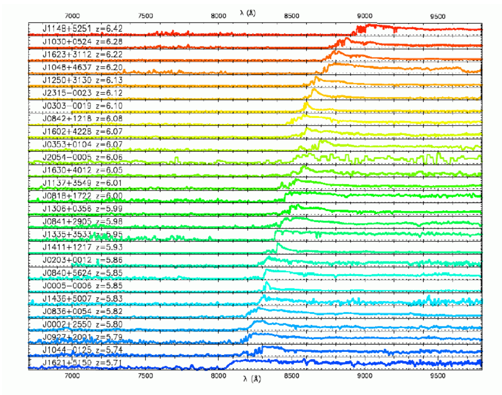

High-z QSOs → latest stages of reionization at z~6-7

& galaxies + GRBs

Constraints on the epoch of reionization

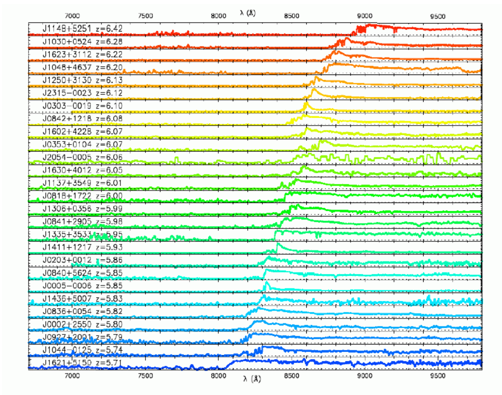

CMB anisotropies

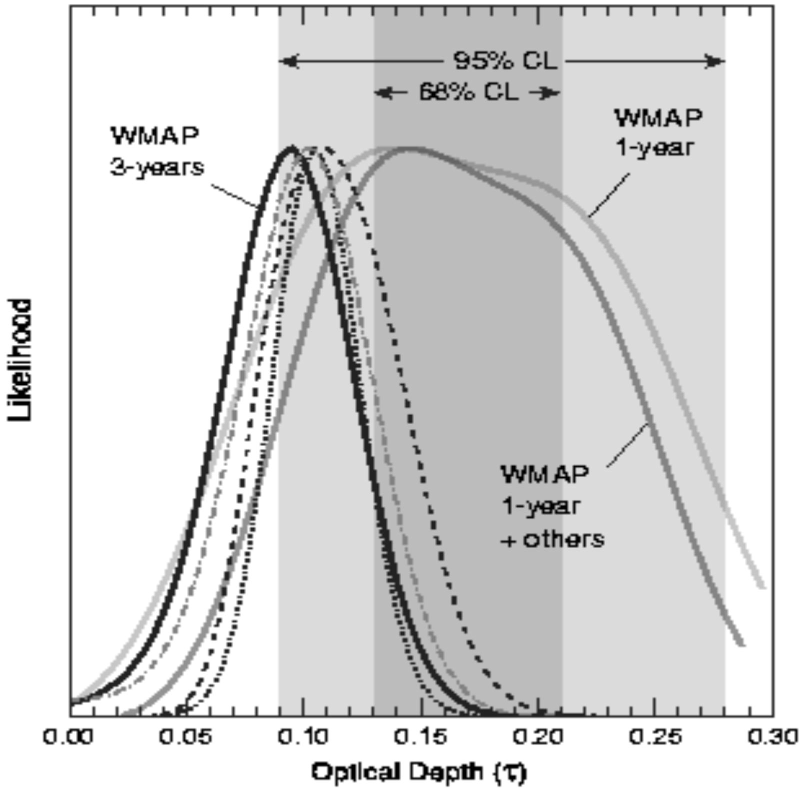

Page+ 2006

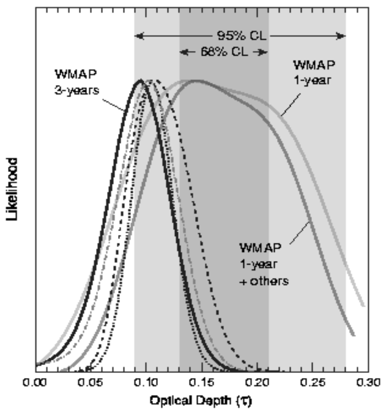

Thomson scattering optical depth: $\tau(z) = \int \ldots n_e(z')\,dz' \propto n_{e,tot}$

$\tau = 0.089 \pm 0.014$ Bennett+ 2013

$\tau = 0.078 \pm 0.019$ Planck Collaboration 2014

Constraints on the epoch of reionization

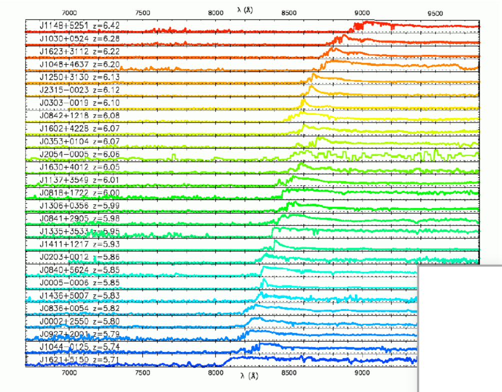

High-z QSOs → latest stages of reionization at z~6-7

How did the reionization process evolve?

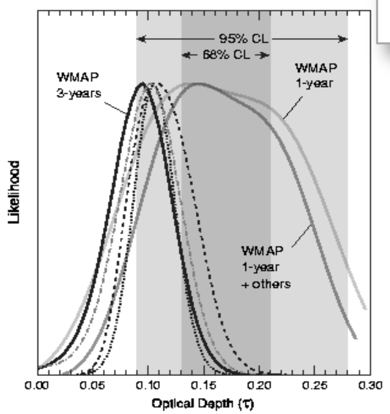

CMB anisotropies → global amount of electrons

Modelling of cosmic reionization: ingredients

Modelling of cosmic reionization: ingredients

✧ Model of galaxy formation

Semi-analytic models

$$M\frac{dn}{dM} = \left(\frac{2}{\pi}\right)^{1/2} \frac{-d(\ln\sigma)}{d(\ln M)} \frac{\rho_0}{M} \upsilon_c e^{-\upsilon_c^2/2}$$

$$\dot{M}_* = \alpha \frac{dM}{dt}$$

$$t_{cool} < t_{dyn}$$

...

+

Numerical simulations

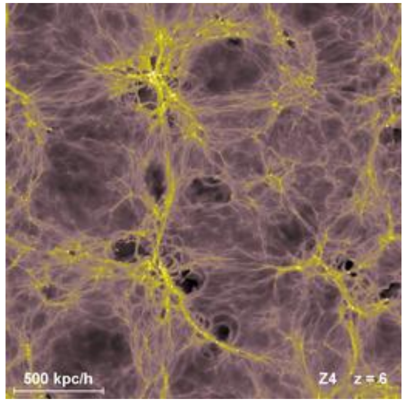

Modelling of cosmic reionization: ingredients

✧ Model of galaxy formation

Semi-analytic models

$$M\frac{dn}{dM} = \left(\frac{2}{\pi}\right)^{1/2} \frac{-d(\ln\sigma)}{d(\ln M)} \frac{\rho_0}{M} \upsilon_c e^{-\upsilon_c^2/2}$$

$$\dot{M}_* = \alpha \frac{dM}{dt}$$

$$t_{cool} < t_{dyn}$$

...

+

Numerical simulations

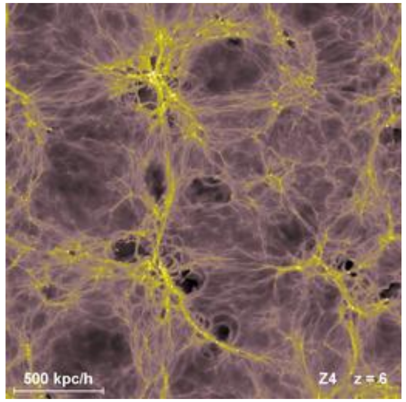

✧ Properties of the sources of ionizing radiation

Stellar type

Quasars

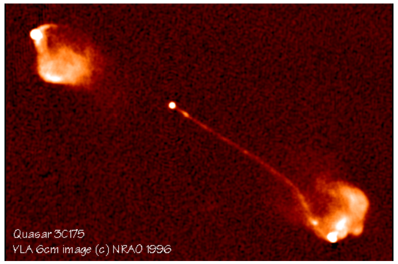

DM annihilation/decay

light dark matter

neutralinos

gravitinos

sterile neutrinos

...

STELLAR TYPE SOURCES

✧ Initial Mass Function and spectrum

Salpeter or Larson IMF?

Zero or higher metallicity?

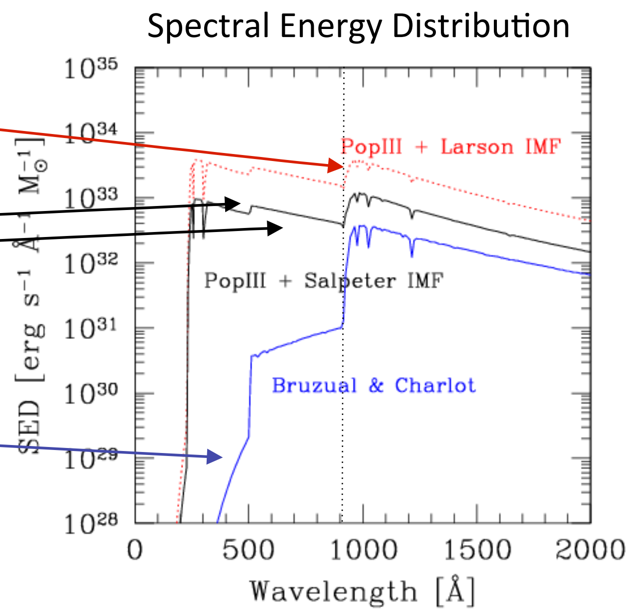

Stellar type sources

✧ Initial Mass Function and spectrum

✧ Primordial (PopIII) → standard (PopII/I) star formation

Stellar type sources

✧ Initial Mass Function and spectrum

✧ Primordial (PopIII) → standard (PopII/I) star formation

✧ Escape fraction

Fesc <20%

Fesc > 70%

Large uncertainties associated
to high-z stellar type sources

QUASARS

✧ Quasars' abundance falls rapidly at high-z

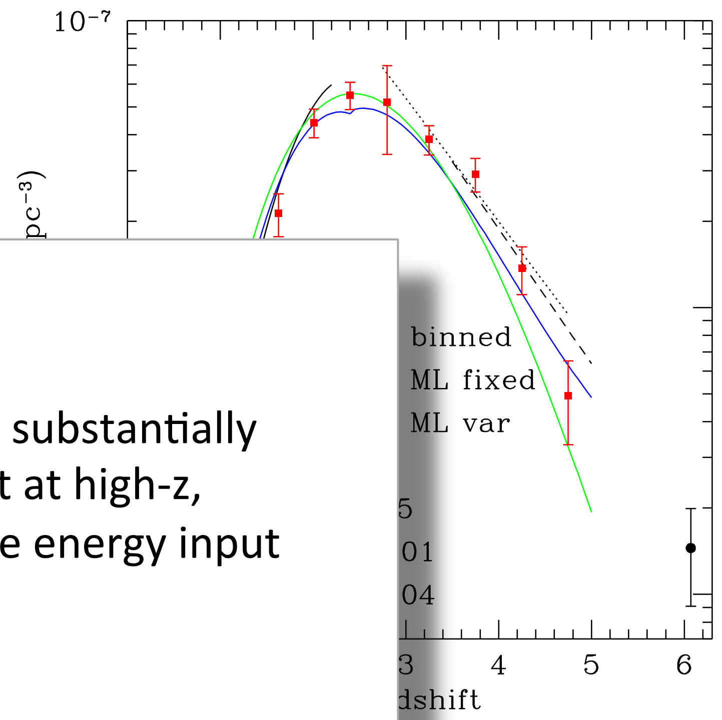

Quasars do not contribute substantially to the ionization budget at high-z, but they could dominate the energy input

Richards+ 2006

✧ HeII late reionization (z~2-3) requires spectral softening with increasing z

Modelling of cosmic reionization: ingredients

✧ Model of galaxy formation

Semi-analytic models

$$M\frac{dn}{dM} = \left(\frac{2}{\pi}\right)^{1/2} \frac{-d(\ln\sigma)}{d(\ln M)} \frac{\rho_0}{M} \upsilon_c e^{-\upsilon_c^2/2}$$

$$\dot{M}_* = \alpha \frac{dM}{dt}$$

$$t_{cool} < t_{dyn}$$

...

+

Numerical simulations

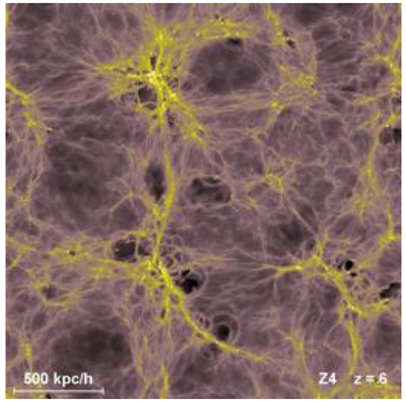

✧ Properties of the sources of ionizing radiation

Stellar type

Quasars

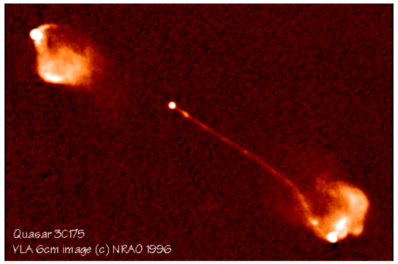

DM annihilation/decay

light dark matter

neutralinos

gravitinos

sterile neutrinos

...

✧ Evolution of the ionized regions

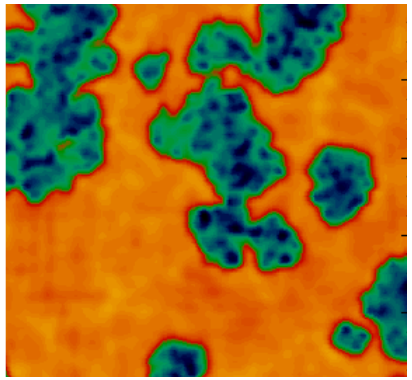

Simulations of H & He reionization

BC, Bolton, Maselli, Graziani 2012

Model of galaxy formation

Gadget-3 simulations from J. Bolton

L [Mpc/h com.]	Particles	Mgas [Msun/h]
35.12	2×512^3	4.15×10^6
8.78	2×256^3	6.48×10^4
4.39	2×256^3	8.11×10^3
2.20	2×256^3	1.01×10^3

Simulations of H & He reionization

BC, Bolton, Maselli, Graziani 2012

Model of galaxy formation

Gadget-3 simulations from J. Bolton

L [Mpc/h com.]	Particles	Mgas [Msun/h]
35.12	2×512^3	4.15×10^6
8.78	2×256^3	6.48×10^4
4.39	2×256^3	8.11×10^3
2.20	2×256^3	1.01×10^3

Properties of the sources of ionizing radiation

Emissivity(z) and distribute it among the halos with power-law spectrum

Index α	% of sources
1.8	100
3 - 1	70 - 30
3	100

Simulations of H & He reionization

BC, Bolton, Maselli, Graziani 2012

Model of galaxy formation

Gadget-3 simulations from J. Bolton

L [Mpc/h com.]	Particles	Mgas [Msun/h]
35.12	2×512^3	4.15×10^6
8.78	2×256^3	6.48×10^4
4.39	2×256^3	8.11×10^3
2.20	2×256^3	1.01×10^3

Properties of the sources of ionizing radiation

Emissivity(z) and distribute it among the halos with power-law spectrum

Index α	% of sources
1.8	100
3 - 1	70 - 30
3	100

Radiative transfer of ionizing photons

CRASH

BC+ 2001; Maselli, Ferrara, BC 2003; Maselli, BC, Kanekar 2009; Pierleoni, Maselli, BC 2009; Partl+ 2011; Graziani, Maselli, BC 2013; Graziani, BC, Ferrara in prep

Simulations of H & He reionization

BC, Bolton, Maselli, Graziani 2012

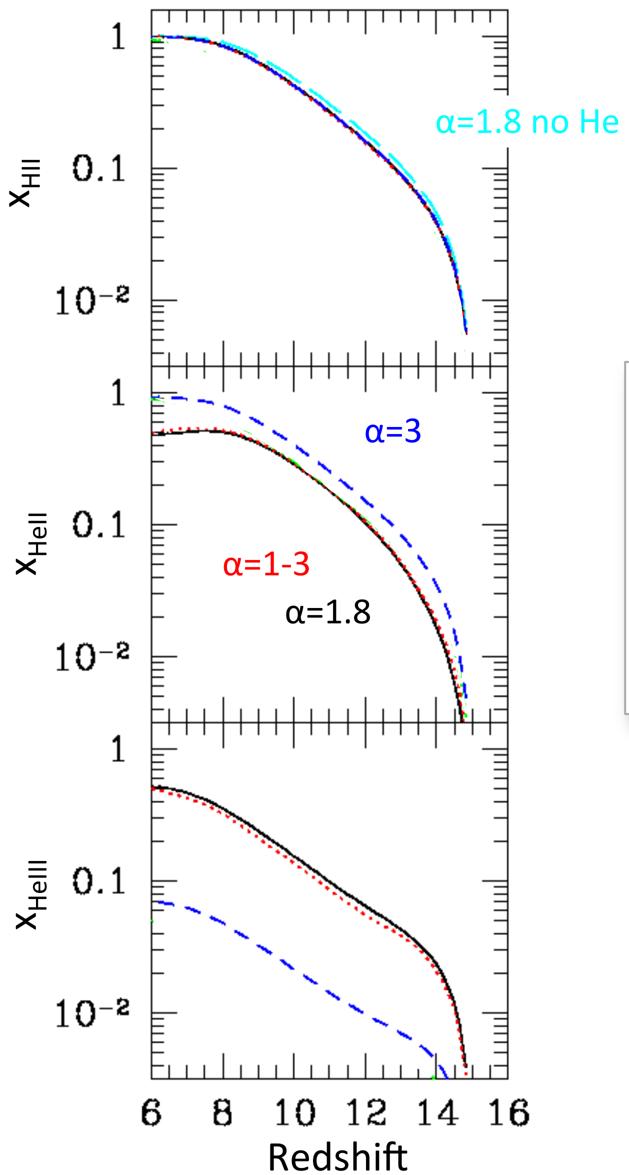

H evolution very similar (independently from He and spectral shape)

He evolution depends on spectral shape

L~35 cMpc/h

Simulations of H & He reionization

BC, Bolton, Maselli, Graziani 2012

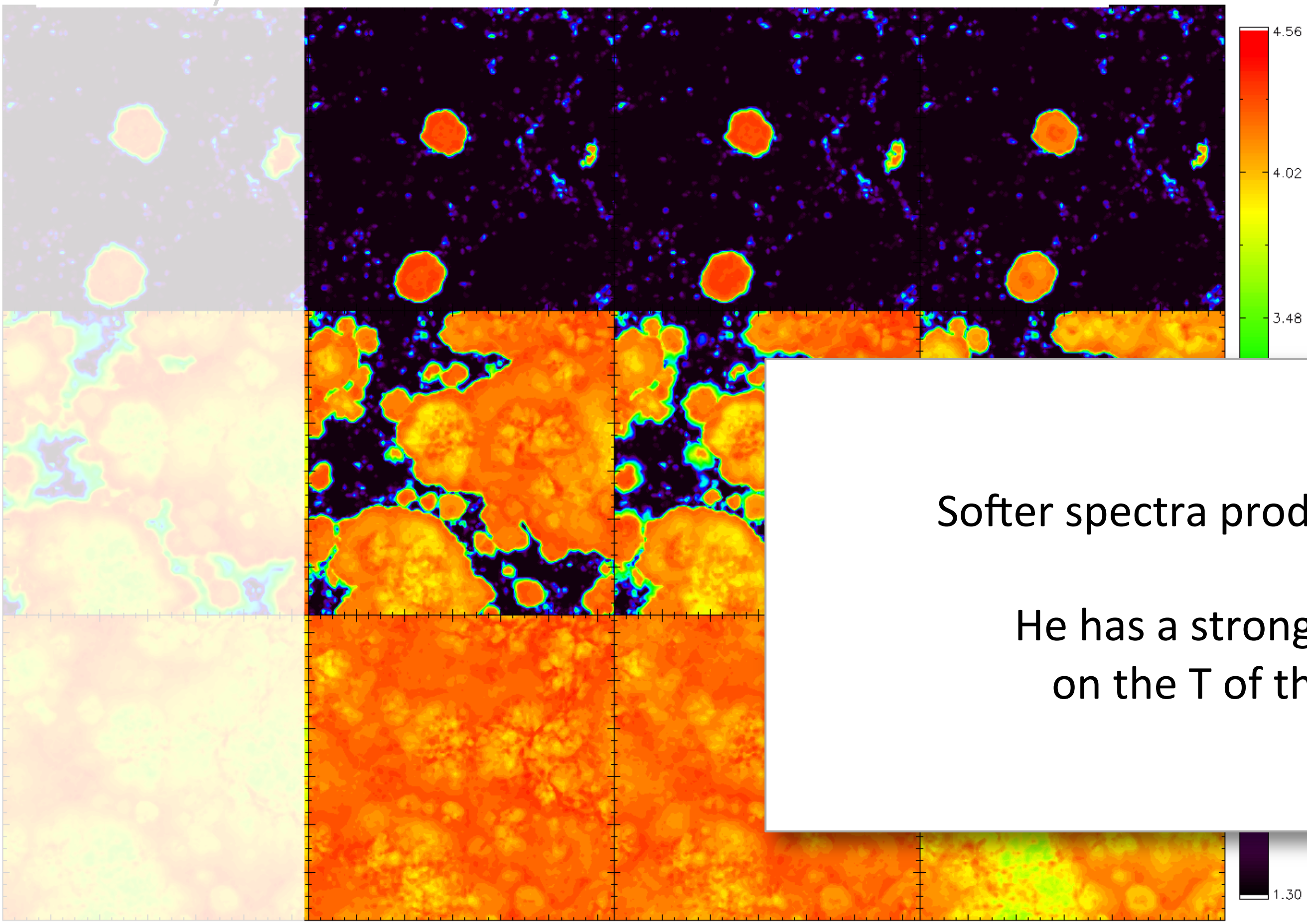

Softer spectra produce lower T

He has a strong impact
on the T of the IGM

21cm line observations

21CM LINE OBSERVATIONS

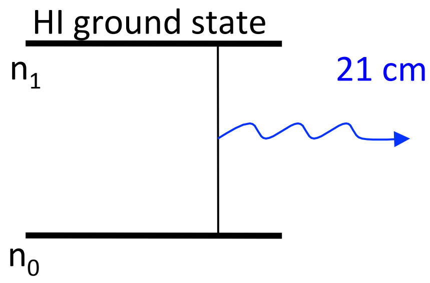

Ideal probe of neutral H at high-z
different observed frqs. → different z

Differential brightness temperature:

$$\delta T_b \approx \frac{T_S - T_{CMB}}{1+z}\tau \propto n_{HI}\left(1 - T_{CMB}/T_S\right)$$

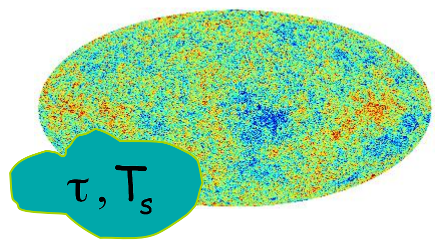

$T_S = T_{CMB} \Rightarrow$ no signal

$T_S < T_{CMB} \Rightarrow$ absorption

$T_S > T_{CMB} \Rightarrow$ emission

The value of T_s is critical

21cm LINE OBSERVATIONS

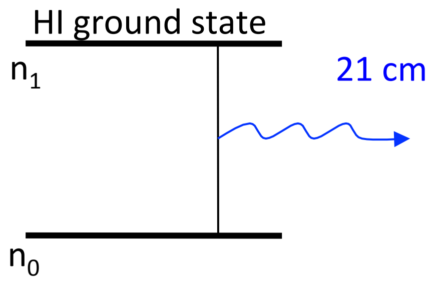

Ideal probe of neutral H at high-z
different observed frqs. → different z

Differential brightness temperature:

$$\delta T_b \approx \frac{T_S - T_{CMB}}{1+z}\tau \propto n_{HI}\left(1 - T_{CMB}/T_S\right)$$

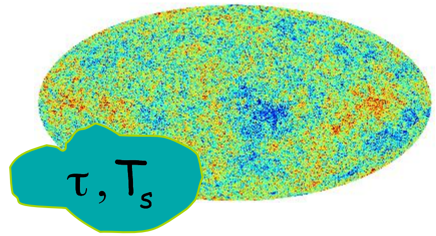

$T_S = T_{CMB} \Rightarrow$ no signal

$T_S < T_{CMB} \Rightarrow$ absorption

$T_S > T_{CMB} \Rightarrow$ emission

kinetic temperature of the gas

$$T_S = \frac{T_{CMB} + (y_\alpha + y_c)T_k}{1 + y_\alpha + y_c}$$

Lyalpha scattering and collisional efficiency

Lyalpha scattering and heating

BC & Salvaterra 2007; BC, Salvaterra, Di Matteo 2009

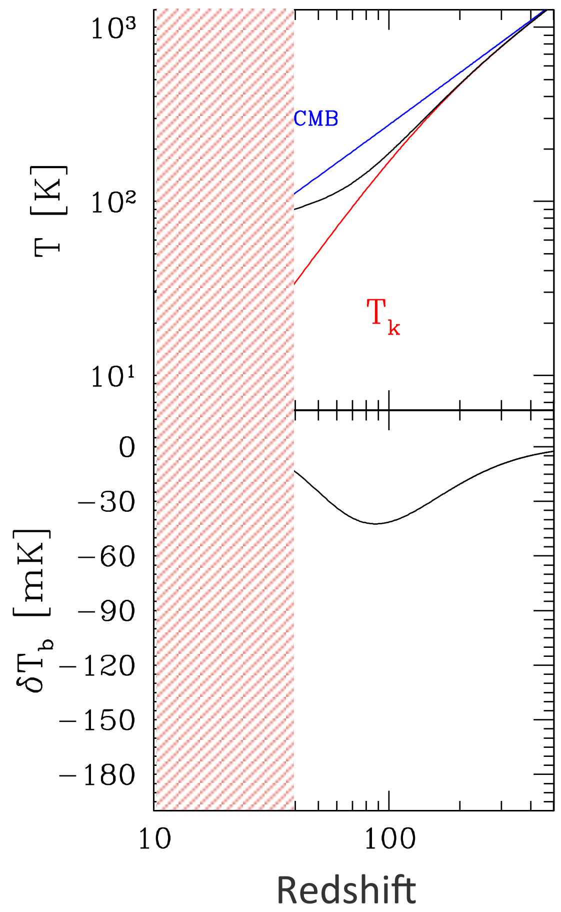

✧ In the absence of decoupling mechanisms, other than collisions, 21cm line will not be visible at z<20

See also e.g. Madau+; Chen & Miralda-Escude ‘;
Chuzoy & Shapiro; Furlanetto+; Mesinger+; Warszawski+

Lyalpha scattering and heating

BC & Salvaterra 2007; BC, Salvaterra, Di Matteo 2009

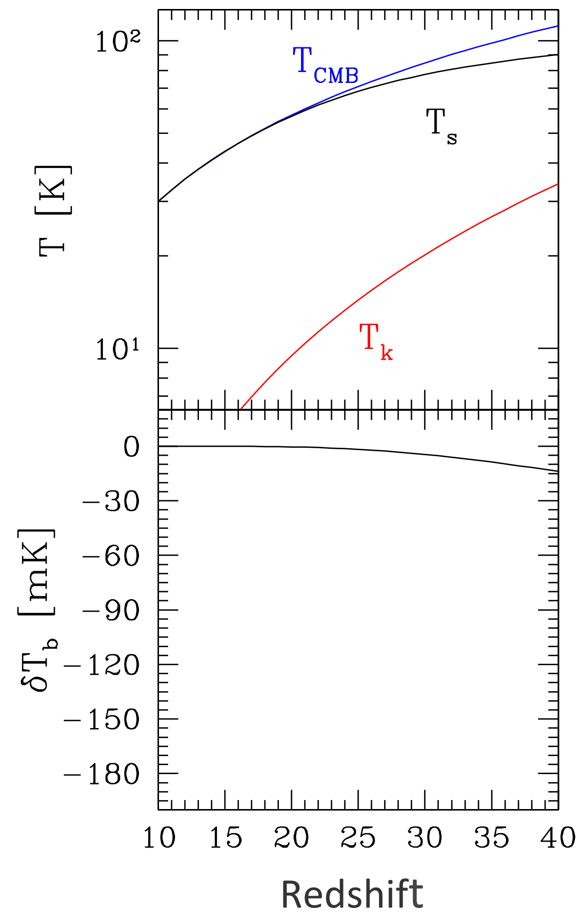

- In the absence of decoupling mechanisms, other than collisions, 21cm line will not be visible at z<20

Lyalpha scattering and heating

BC & Salvaterra 2007; BC, Salvaterra, Di Matteo 2009

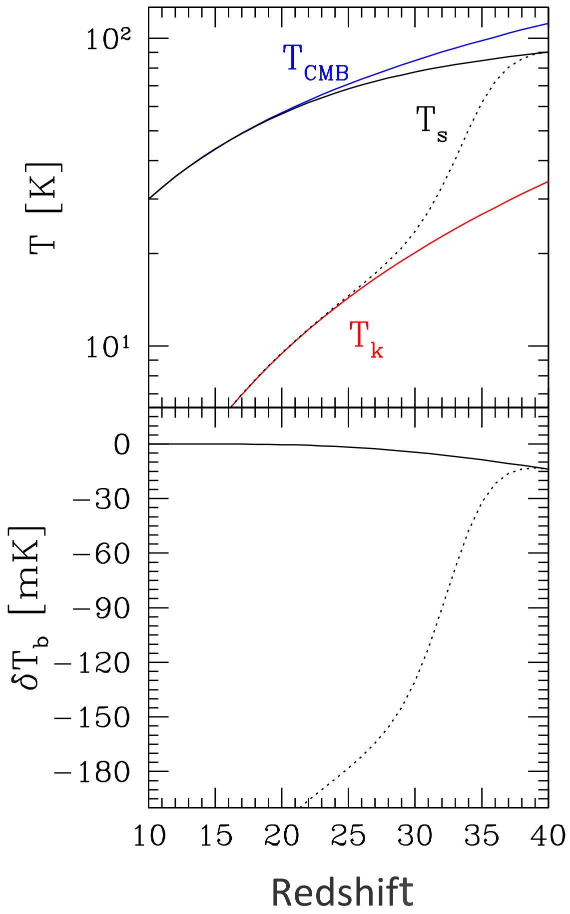

✧ In the absence of decoupling mechanisms, other than collisions, 21cm line will not be visible at z<20

✧ Lyα photon scattering decouples T_s from T_{CMB} → 21cm line can be observed

LYALPHA SCATTERING AND HEATING

BC & Salvaterra 2007; BC, Salvaterra, Di Matteo 2009

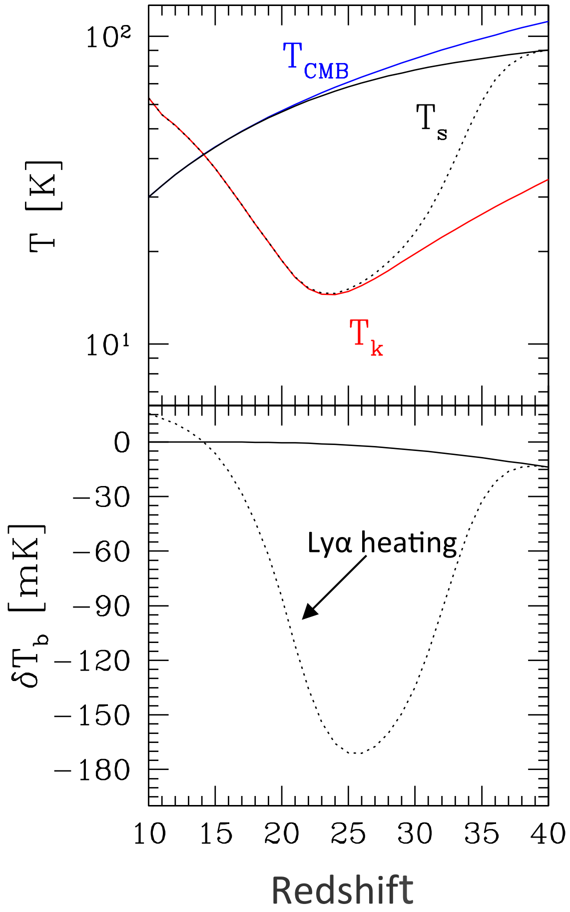

- In the absence of decoupling mechanisms, other than collisions, 21cm line will not be visible at z<20
- Lyα photon scattering decouples T_S from T_{CMB} → 21cm line can be observed
- Lyα photon scattering heats the gas → 21cm line can be observed in emission

$$\delta T_b \approx n_{HI}(1 - T_{CMB}/T_S)$$

$$T_S >> T_{CMB} \rightarrow \delta T_b \approx n_{HI}$$

21cm line observations

21cm line observations

✧ *Tomography:* topology of HII regions; information on sources; when reionization occurred

e.g. Tozzi+ 2000; BC & Madau 2003; Furlanetto, Sokasian, Hernquist 2004;
Mellema+ 2006; Valdes+ 2006; Santos+ 2008; Baek+ 2009;
Geil & Wyithe 2009; Zaroubi+ 2012; Malloy & Lidz 2013

21cm line observations

✧ *Tomography:* topology of HII regions; information on sources; when reionization occurred

e.g. Tozzi+ 2000; BC & Madau 2003; Furlanetto, Sokasian, Hernquist 2004;
Mellema+ 2006; Valdes+ 2006; Santos+ 2008; Baek+ 2009;
Geil & Wyithe 2009; Zaroubi+ 2012; Malloy & Lidz 2013

✧ *δT_b fluctuations and Power Spectrum:* statistical estimates

e.g. Madau, Meiksin & Rees 1997; Shaver+ 1999; Tozzi+ 2000; BC & Madau 2003;
Furlanetto, Sokasian, Hernquist 2004; Mellema+ 2006; Valdes+ 2006; Datta+ 2008;
Pritchard & Loeb 2008; Santos+ 2008; Baek+ 2009; Geil & Wyithe 2009

21cm line observations

✧ *Tomography:* topology of HII regions; information on sources; when reionization occurred

e.g. Tozzi+ 2000; BC & Madau 2003; Furlanetto, Sokasian, Hernquist 2004;
Mellema+ 2006; Valdes+ 2006; Santos+ 2008; Baek+ 2009;
Geil & Wyithe 2009; Zaroubi+ 2012; Malloy & Lidz 2013

✧ δT_b *fluctuations and Power Spectrum:* statistical estimates

e.g. Madau, Meiksin & Rees 1997; Shaver+ 1999; Tozzi+ 2000; BC & Madau 2003;
Furlanetto, Sokasian, Hernquist 2004; Mellema+ 2006; Valdes+ 2006; Datta+ 2008;
Pritchard & Loeb 2008; Santos+ 2008; Baek+ 2009; Geil & Wyithe 2009

✧ *21cm forest:* information on HI along the l.o.s.

e.g. Carilli, Gnedin & Owen 2002; Furlanetto 2006;
Xu+ 2009; Mack & Wyithe 2011; Meiksin 2011;
Xu, Ferrara & Chen 2011; BC+ 2013;
Vasiliev & Shchekinov 2012; Ewall-Wice at al. 2014

21cm line observations

✧ *Tomography:* topology of HII regions; information on sources; when reionization occurred

e.g. Tozzi+ 2000; BC & Madau 2003; Furlanetto, Sokasian, Hernquist 2004;
Mellema+ 2006; Valdes+ 2006; Santos+ 2008; Baek+ 2009;
Geil & Wyithe 2009; Zaroubi+ 2012; Malloy & Lidz 2013

✧ *δT_b fluctuations and Power Spectrum:* statistical estimates

e.g. Madau, Meiksin & Rees 1997; Shaver+ 1999; Tozzi+ 2000; BC & Madau 2003;
Furlanetto, Sokasian, Hernquist 2004; Mellema+ 2006; Valdes+ 2006; Datta+ 2008;
Pritchard & Loeb 2008; Santos+ 2008; Baek+ 2009; Geil & Wyithe 2009

✧ *21cm forest:* information on HI along the l.o.s.

e.g. Carilli, Gnedin & Owen 2002; Furlanetto 2006;
Xu+ 2009; Mack & Wyithe 2011; Meiksin 2011;
Xu, Ferrara & Chen 2011; BC+ 2013;
Vasiliev & Shchekinov 2012; Ewall-Wice at al. 2014

✧ *Cross-correlation:* information on typical dimension of HII regions

Salvaterra+ 2005; Lidz+ 2009; Jelic+ 2010;
Wiersma+ 2013; Fernandez+2013

LOFAR: LOw FREQUENCY ARRAY

LBA (10) 20 - 80 MHz

isolated dipoles

HBA 115 - 240 MHz

tiles (4x4 dipoles)

A station has 24/48/96 dipoles/tiles

Core:	2 km	18+ stations
Netherlands:	80 km	18+ stations
Europe:	>1000 km	9+ stations

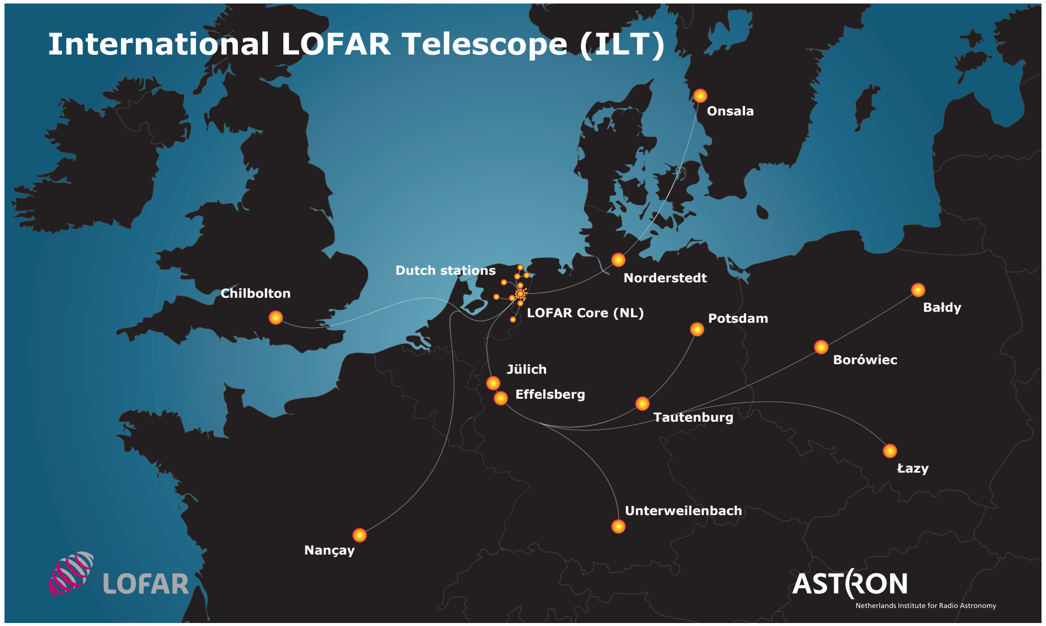

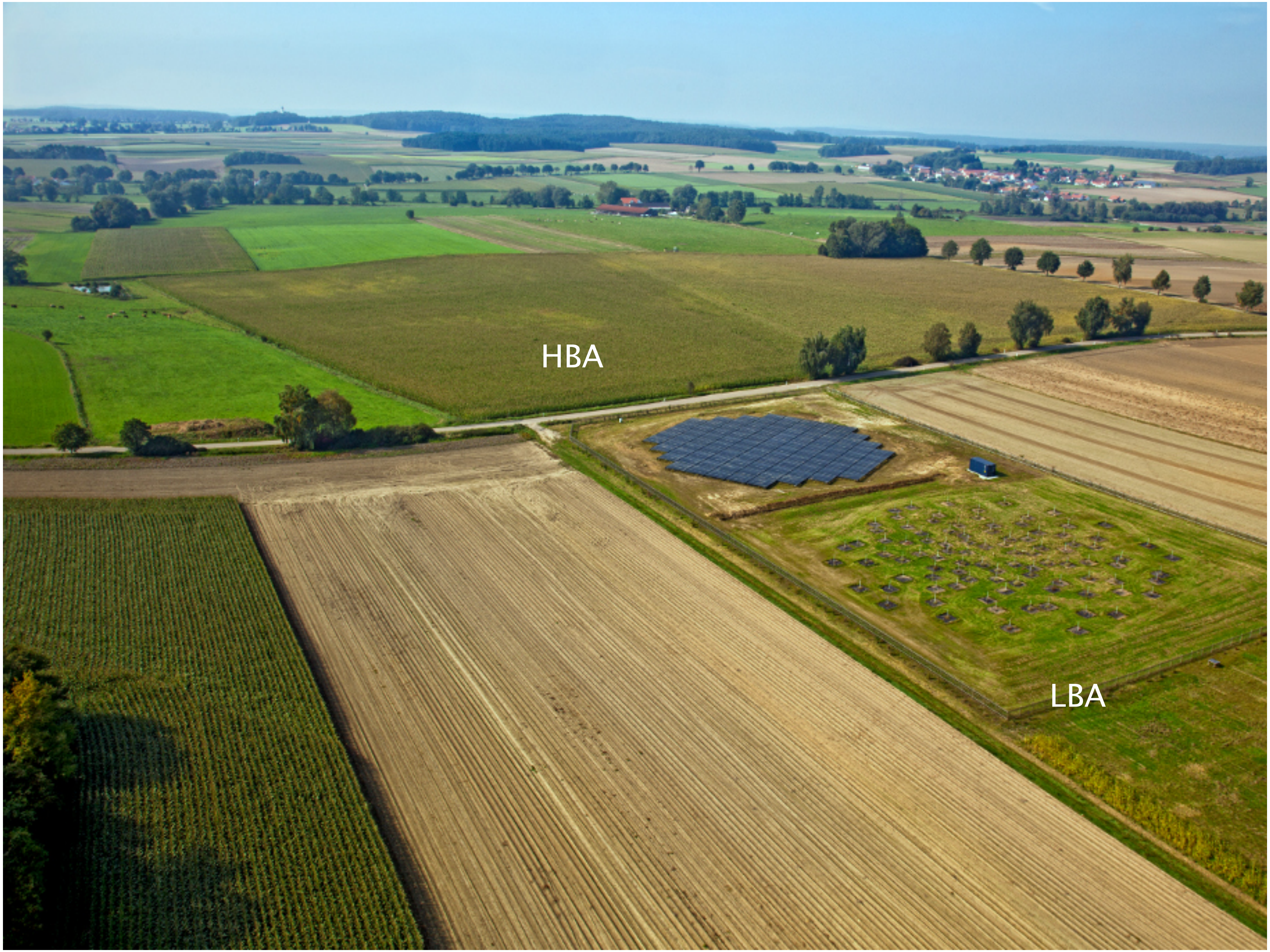
HBA
LBA


© 2011 Geocentre Consulting
Image © 2011 GeoBasis-DE/BKG
© 2011 PPWK
© 2011 Tele Atlas
Google earth

Simulations for LOFAR

✧ Semi-numeric approach

CRASH

BC+ 2001;
Maselli, Ferrara & BC 2003;
Maselli, BC & Kanekar 2009;
Partl+ 2011;
Graziani, Maselli, BC 2013

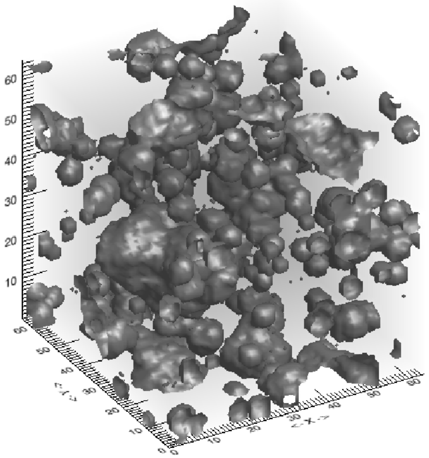

12.5 Mpc/h com.

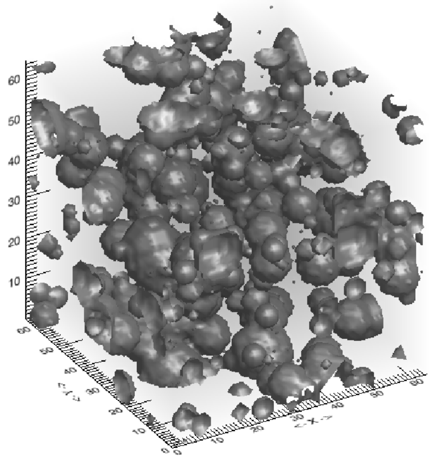

12.5 Mpc/h com.

BEAR

Thomas & Zaroubi 2008

Thomas+ 2009

Simulations for LOFAR

✧ Semi-numeric approach

Semi-numeric approaches are typically appropriate for studies of 21cm signal

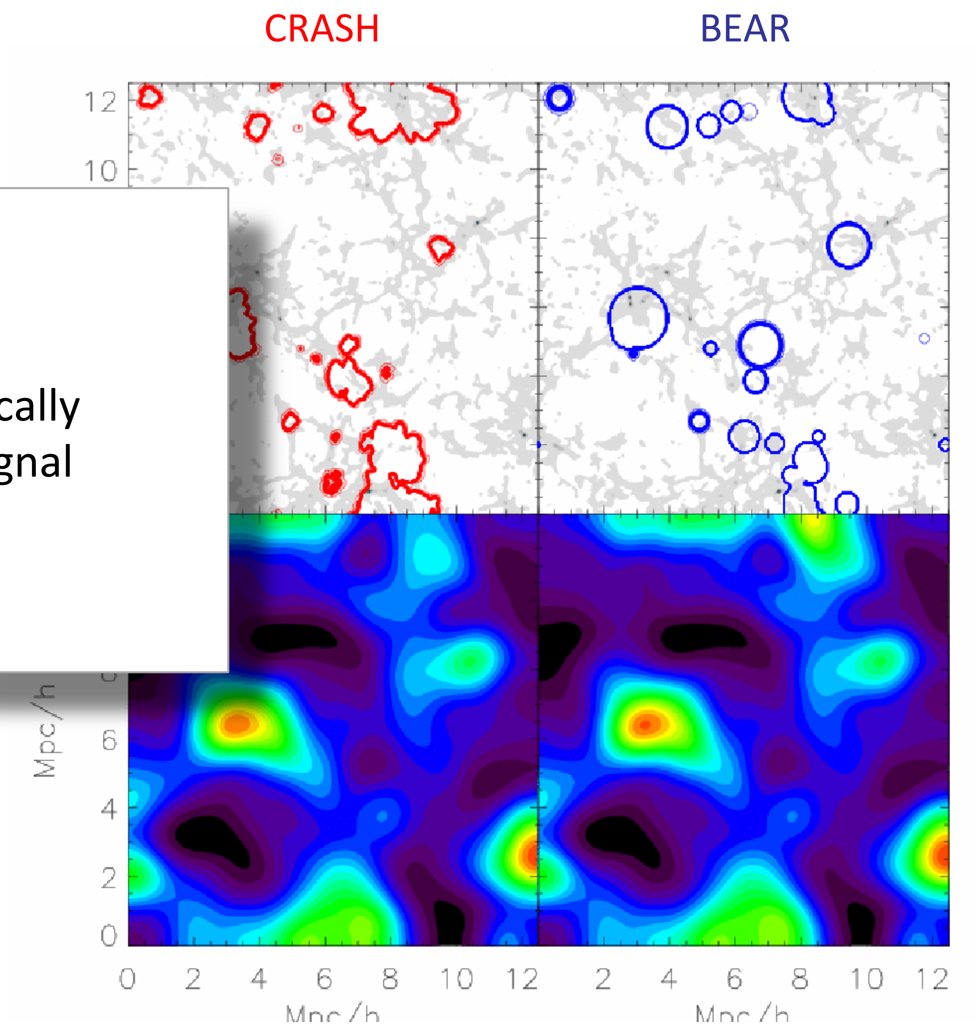

Thomas+ 2009

Imaging with LOFAR

Zaroubi+ 2012

600 cMpc
box with 21cmFast

A +
20arcmin smoothing

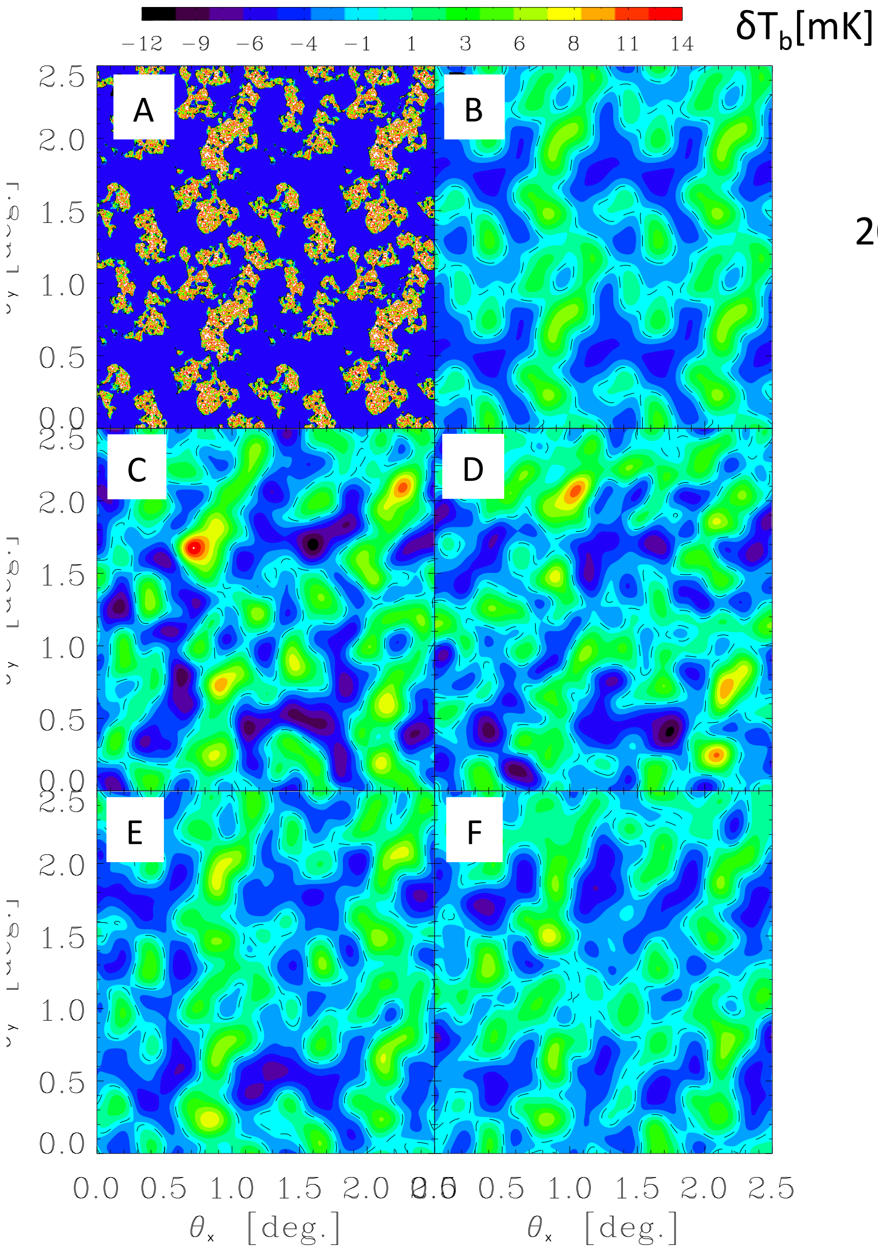

B +
noise 600h

C + -
foregrounds

as C for 2400h

as D for 2400h

Imaging with LOFAR

Zaroubi+ 2012

600 cMpc
box with 21cmFast

A +
20arcmin smoothing

B +
noise 600h

C + -
foregrounds

as C for 2400h

as D for 2400h

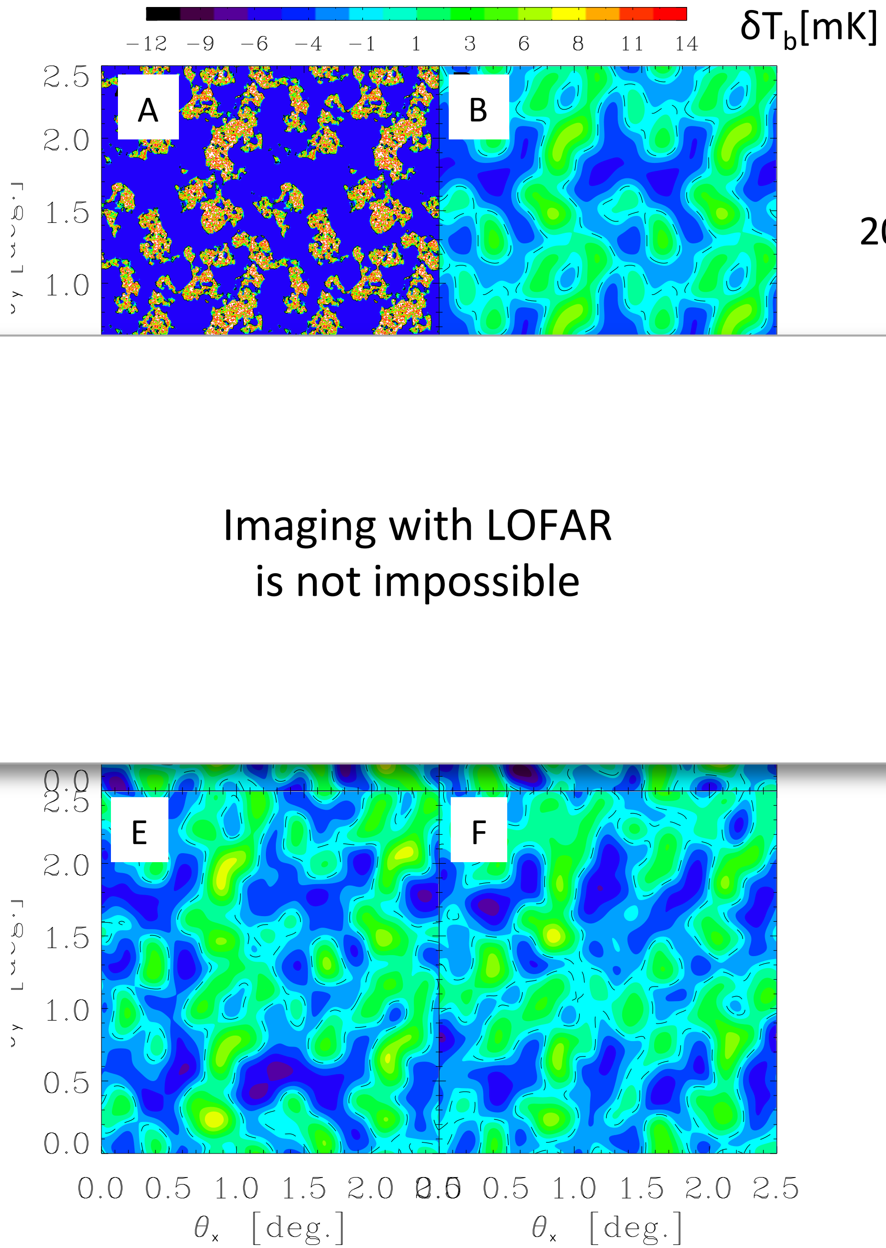

Imaging with LOFAR
is not impossible

Imaging with LOFAR: QSOs' ionized regions

Imaging with LOFAR: QSOs' ionized regions

Kakiichi+ in prep

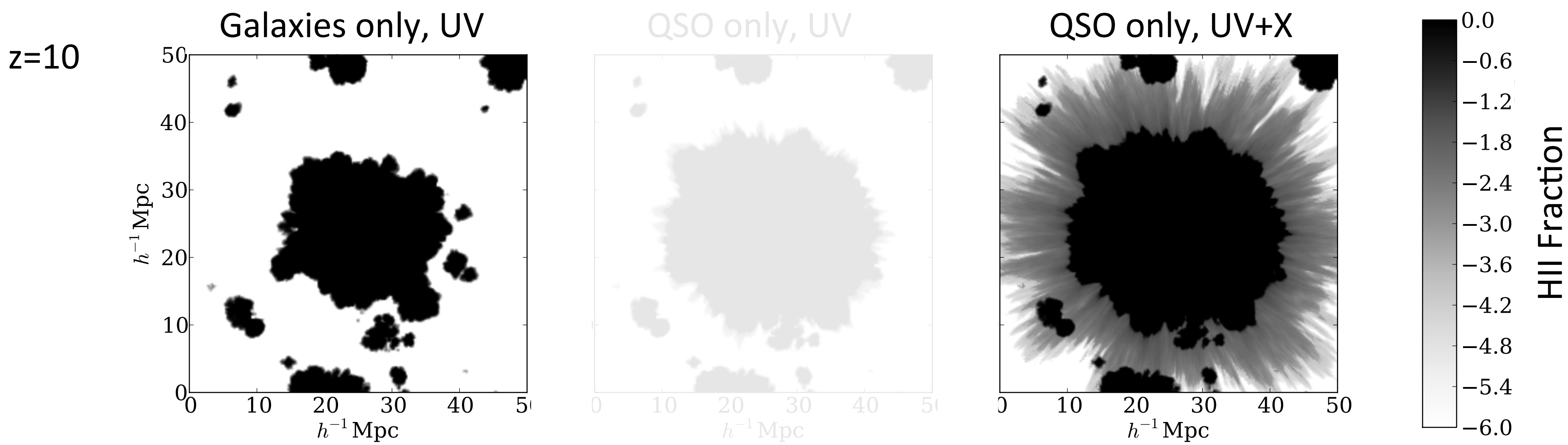

When QSO is on it dominates ionization budget.

X-rays produce partially ionized shell.

Not possible to distinguish QSO vs galaxies.

Imaging with LOFAR: QSOs' ionized regions

Kakiichi+ in prep

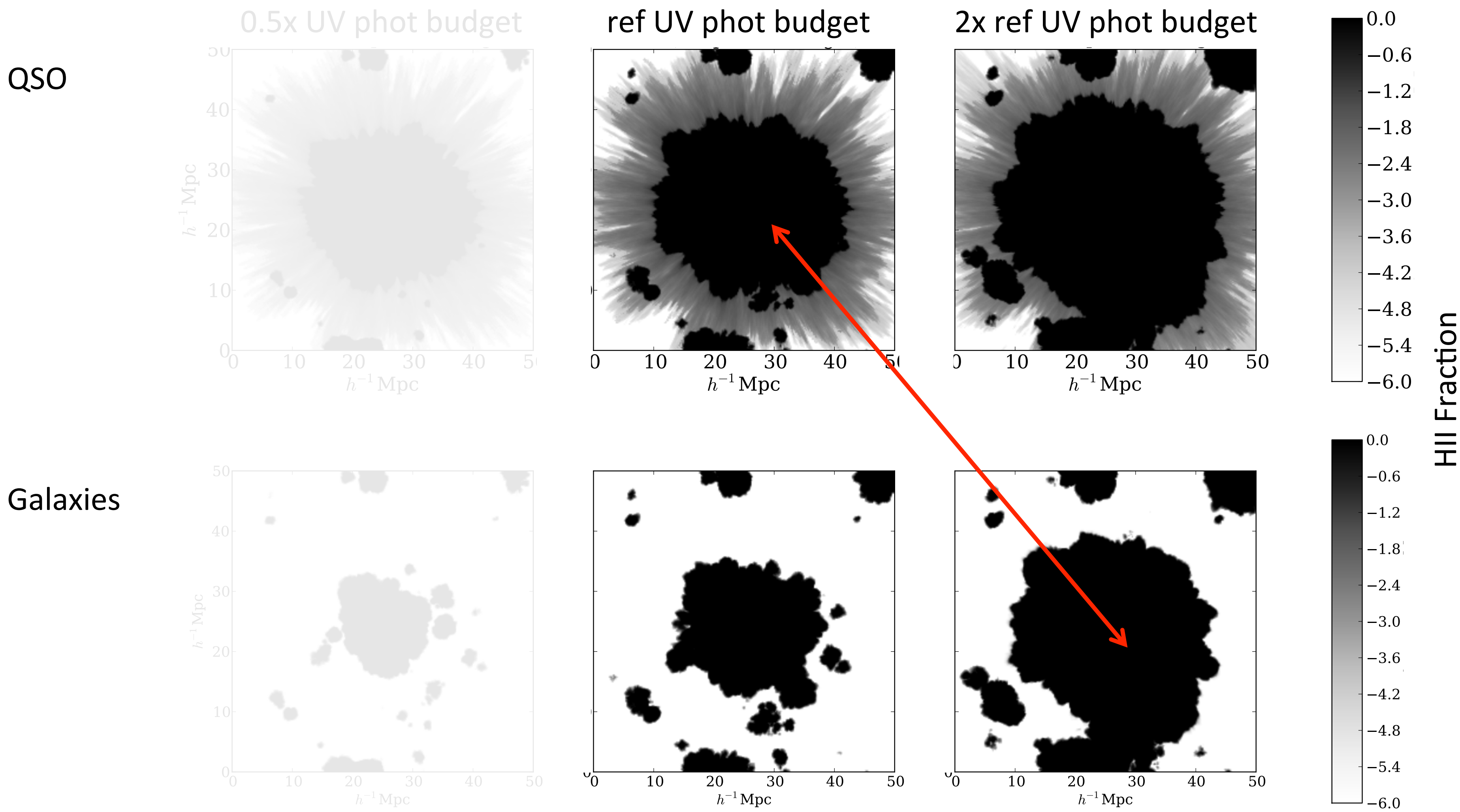

z=10

Imaging with LOFAR: QSOs' ionized regions

Kakiichi+ in prep

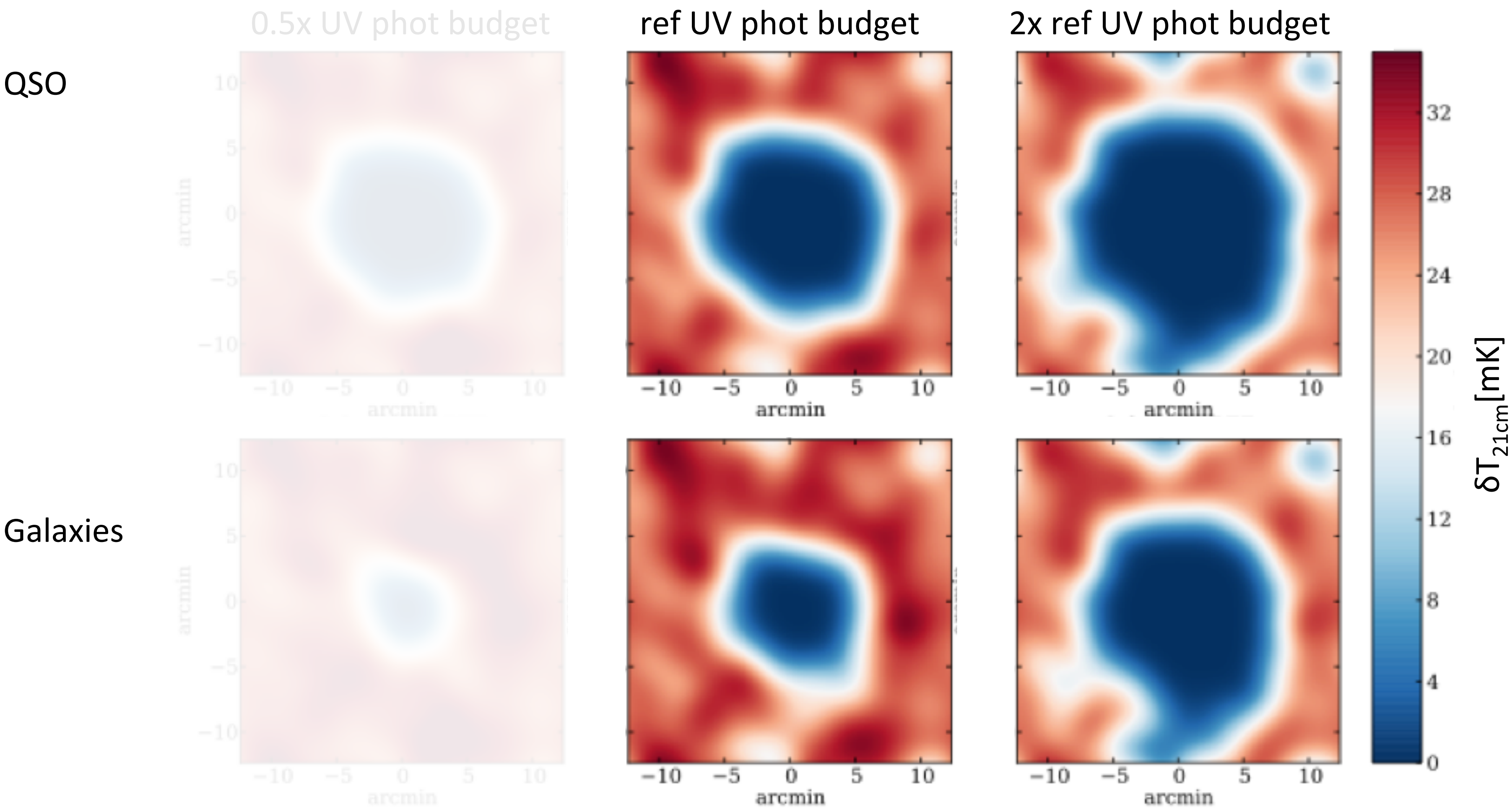

z=10

Imaging with LOFAR: QSOs' ionized regions

Kakiichi+ in prep

Reionization

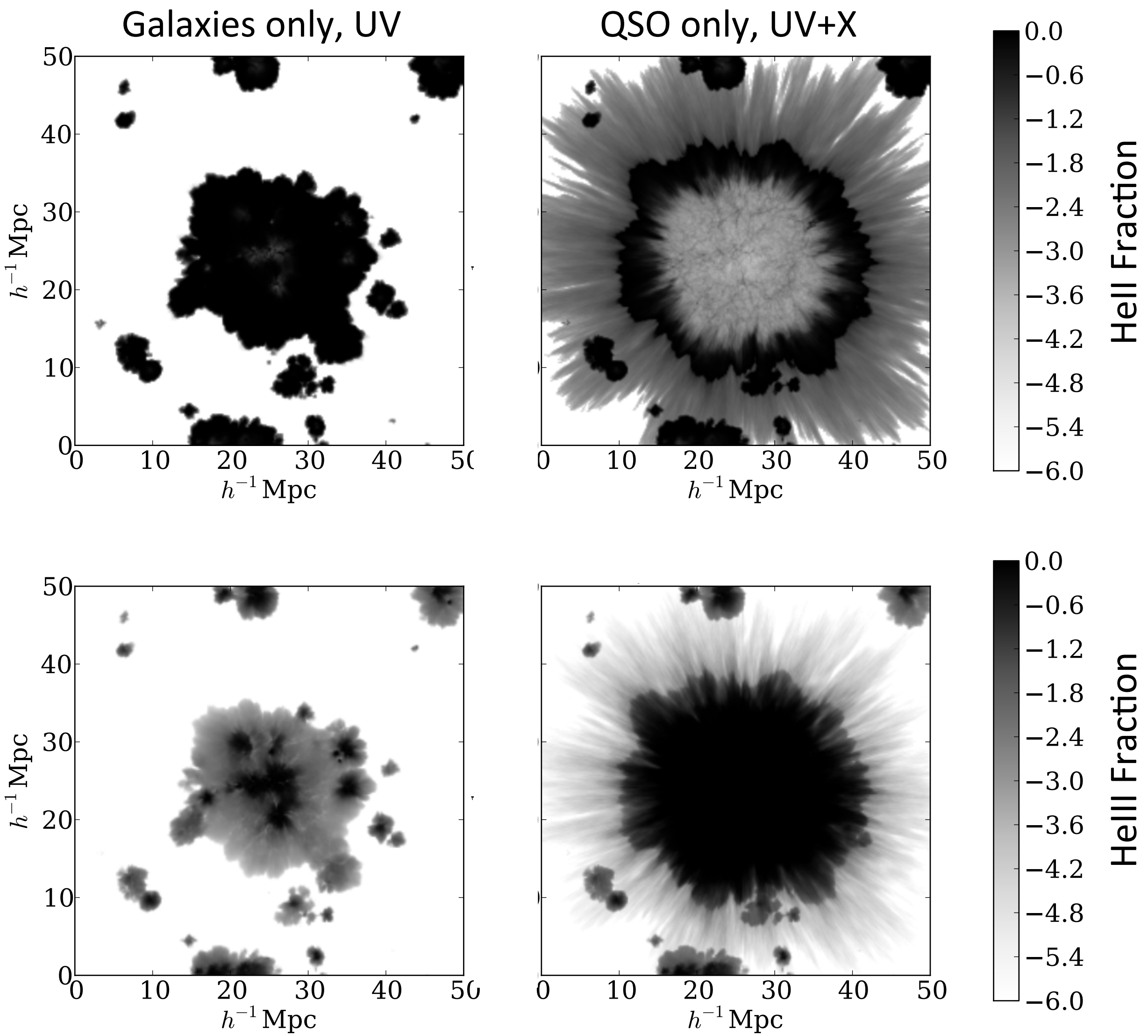

z=10

Imaging with LOFAR: QSOs' ionized regions

Kakiichi+ in prep

Reionization

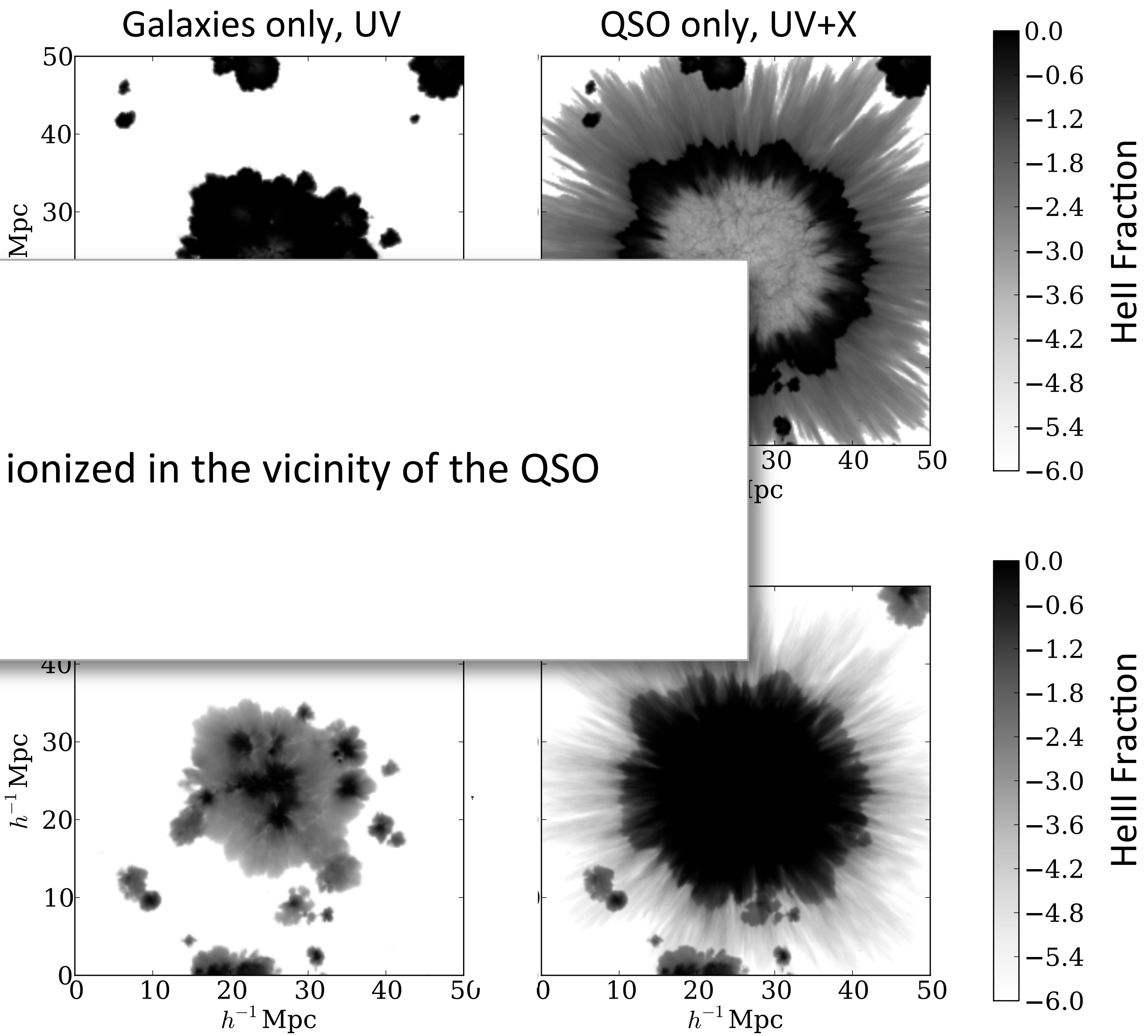

He is fully ionized in the vicinity of the QSO

z=10

Statistical measures with LOFAR

Patil+ 2014

Variance of the signal

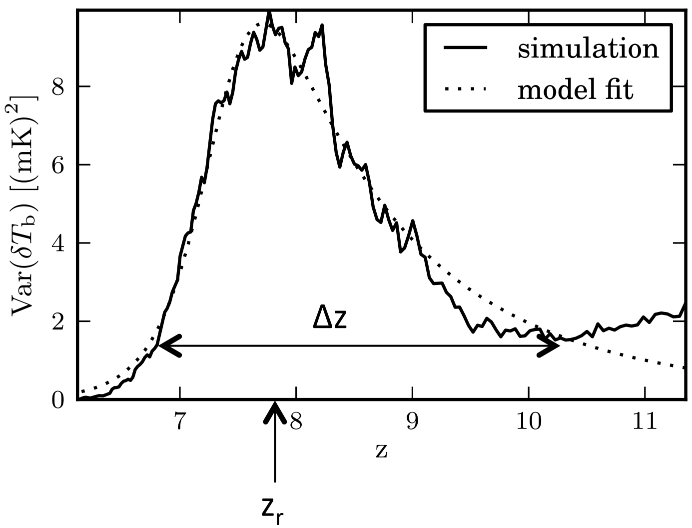

- ✧ Simulation in 600 cMpc with 21cmFast
- ✧ $\mathrm{Var}(\delta T_b)=\langle P[k] \rangle$ fitted with 2 parameters model: z_r and Δz
- ✧ Foregrounds, instrumental response, noise (600h) → simulated data
- ✧ Signal variance is extracted from simulated data
- ✧ Estimate best fitting parameters

Statistical measures with LOFAR

Patil+ 2014

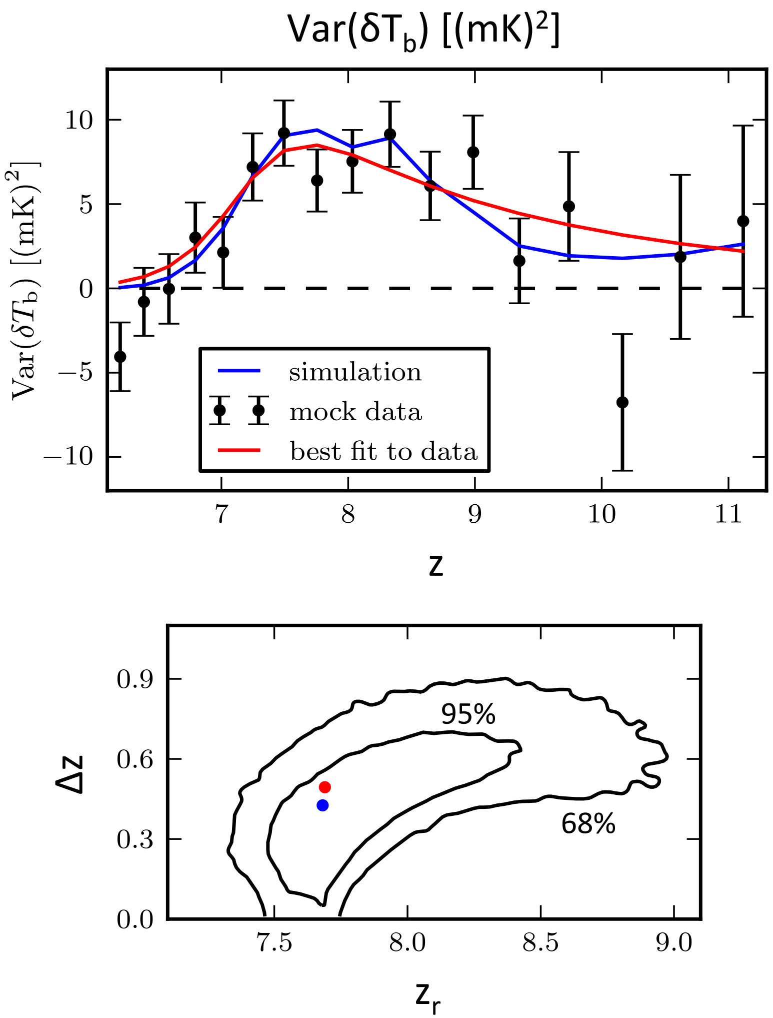

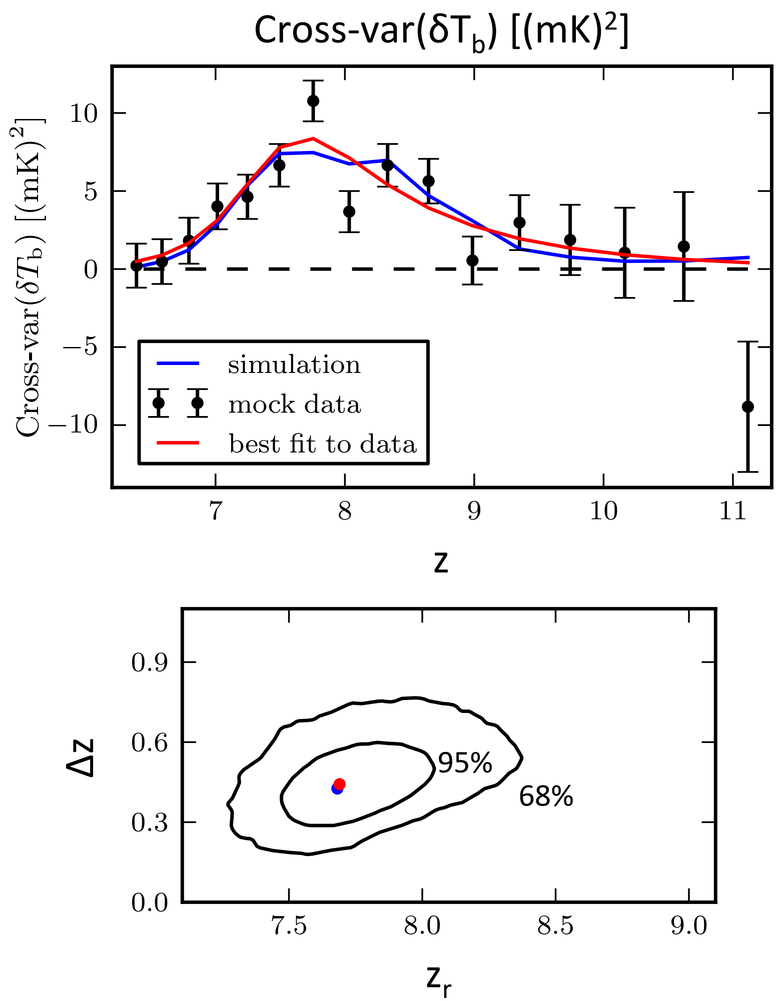

Statistical measures with LOFAR

Patil+ 2014

z_r=7.68, Δz=0.43

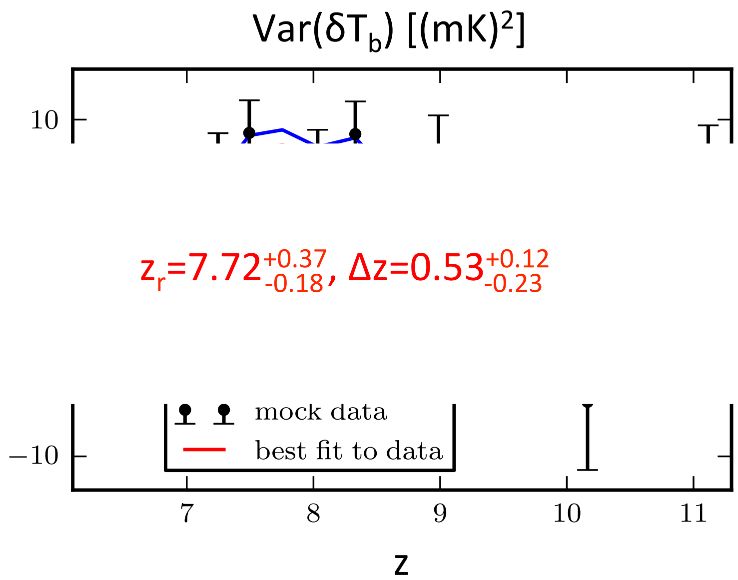

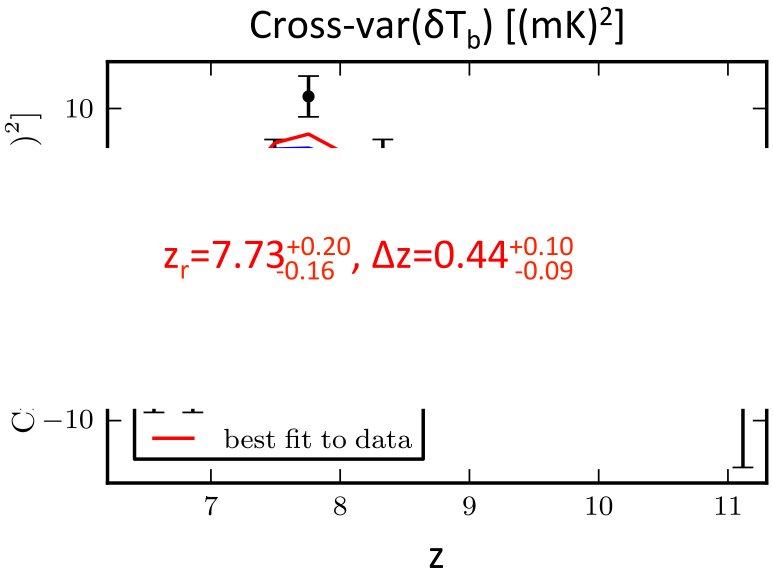

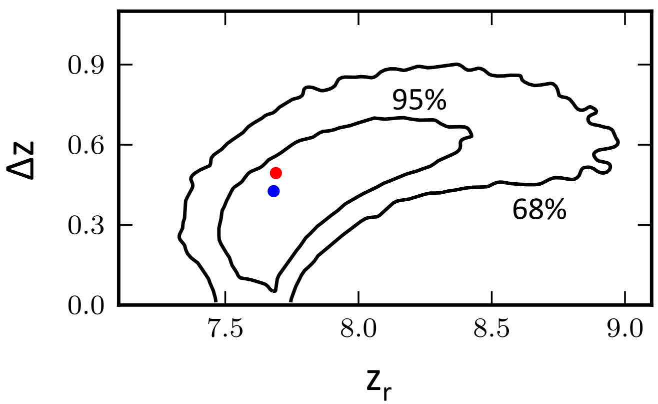

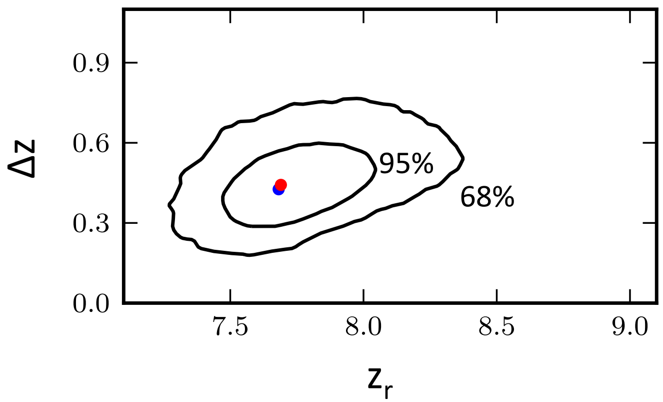

Statistical measures with LOFAR

Patil+ 2014

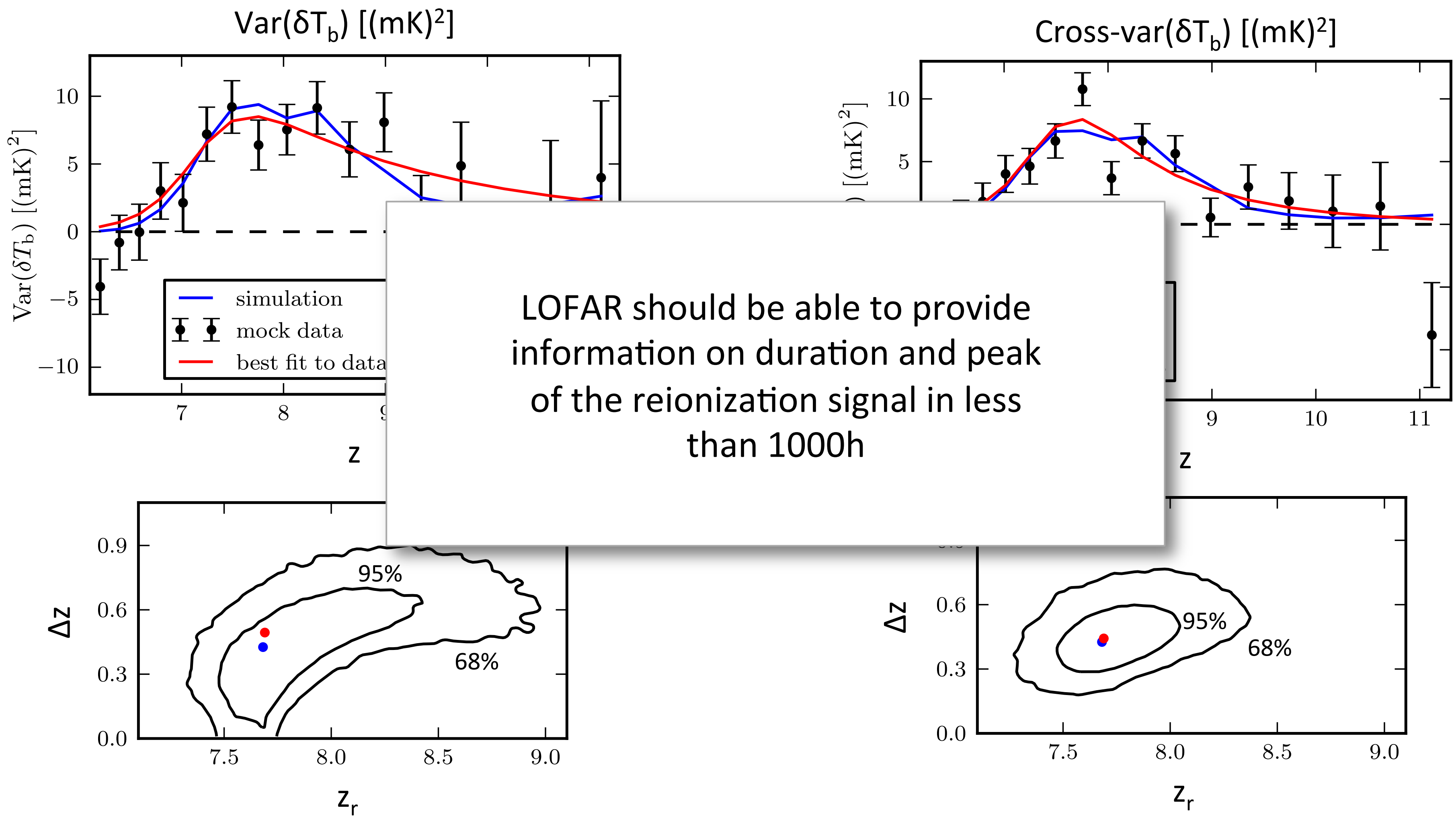

LOFAR should be able to provide information on duration and peak of the reionization signal in less than 1000h

The 21cm forest

BC+ 2012

$$\tau_{21cm} \propto x_{HI}(1+\delta)\frac{1}{T_s}$$

THE 21CM FOREST

BC+ 2012

z=10, S=50 mJy, α=1.05

BW=10 kHz, s=10 kHz, t=1000 h

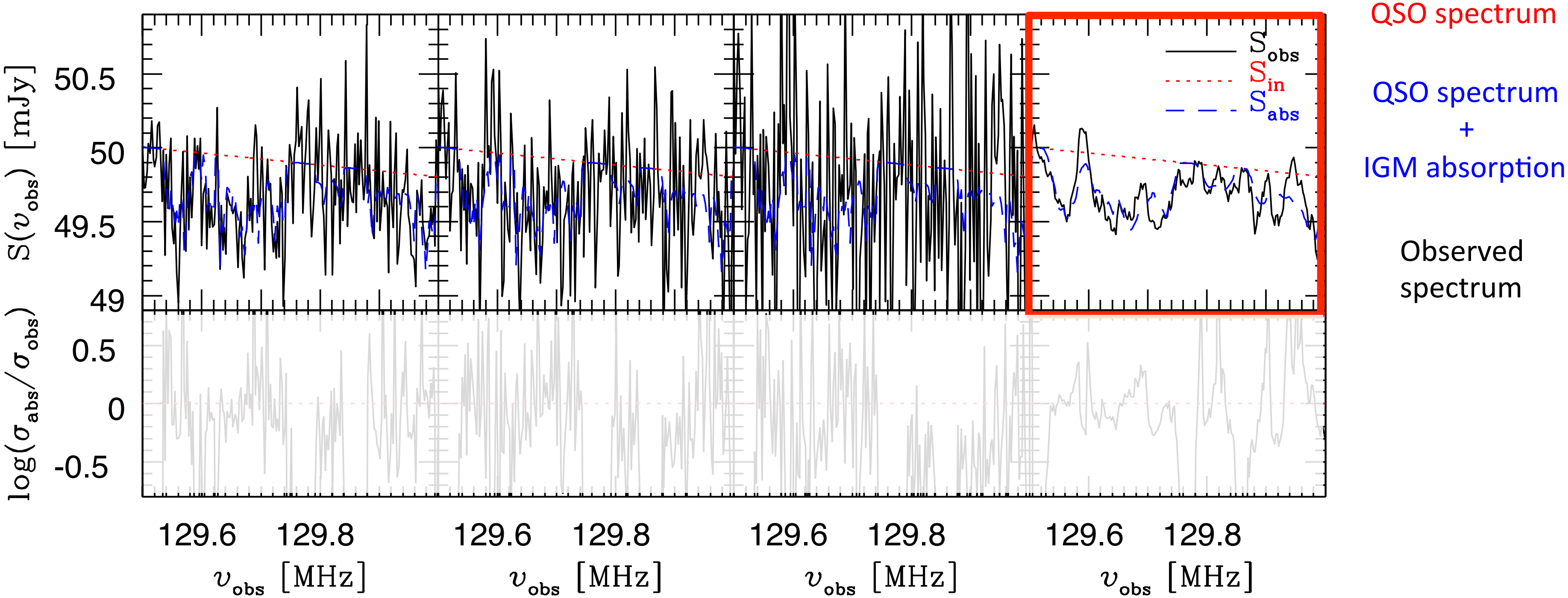

$\sigma = S - S_{in}$

The 21cm forest

BC+ 2012

z=7.6, S=50 mJy, α=1.05

BW=5 kHz, s=5 kHz, t=1000 h

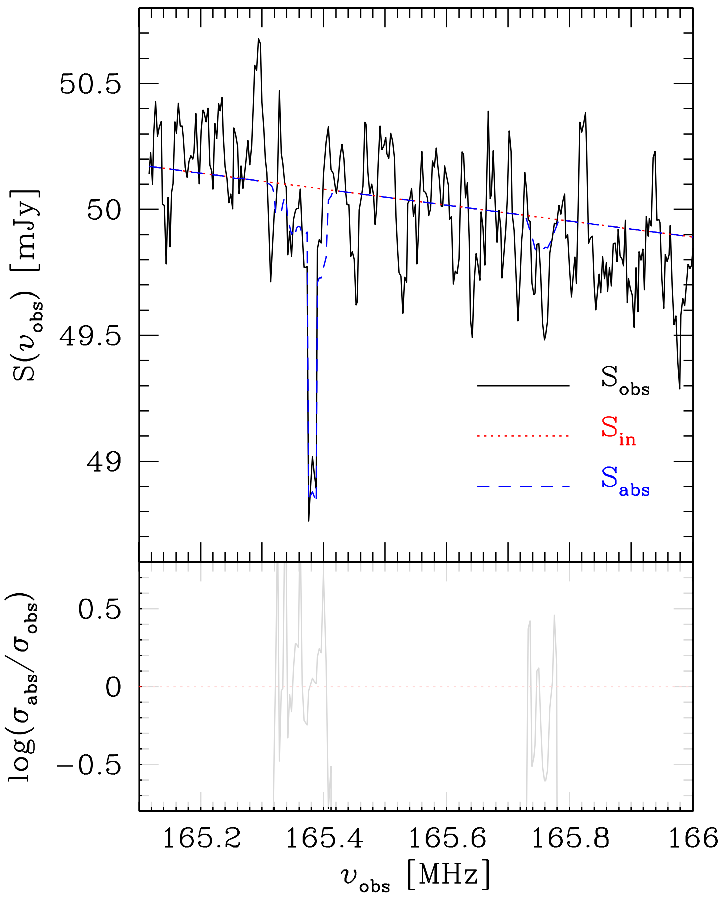

QSO spectrum

QSO spectrum
+
IGM absorption

Observed
spectrum

The 21cm forest

BC+ 2012

z=7.6, S=50 mJy, α=1.05

BW=5 kHz, s=5 kHz, t=1000 h

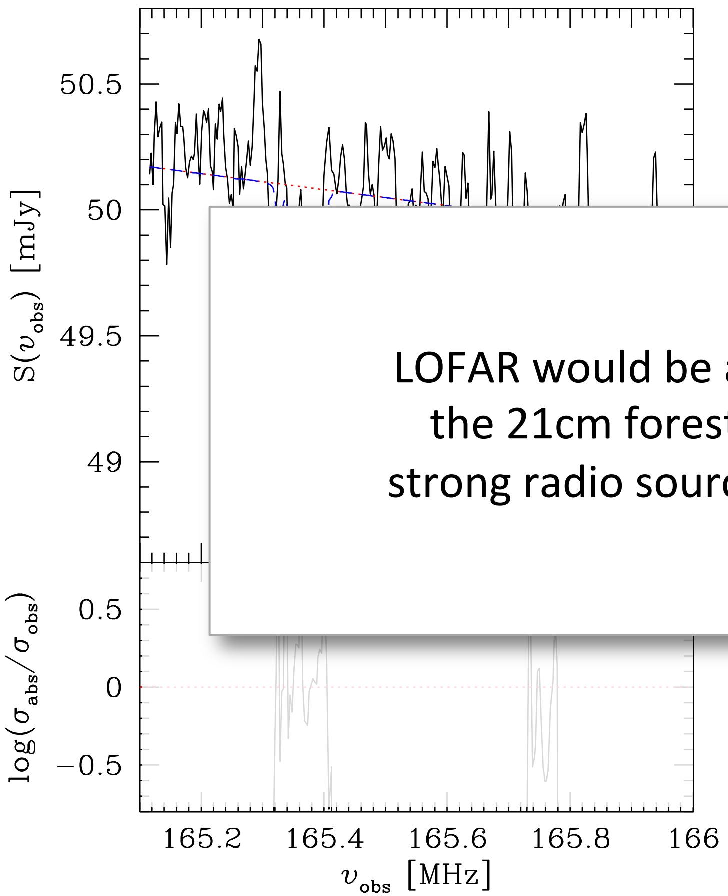

QSO spectrum

QSO spectrum
+
IGM absorption

...served
...ectrum

LOFAR would be able to detect the 21cm forest IF a high-z, strong radio source were found

Cross-correlation 21cm-galaxy surveys

Wiersma+ 2013; Vrbanec+ in prep

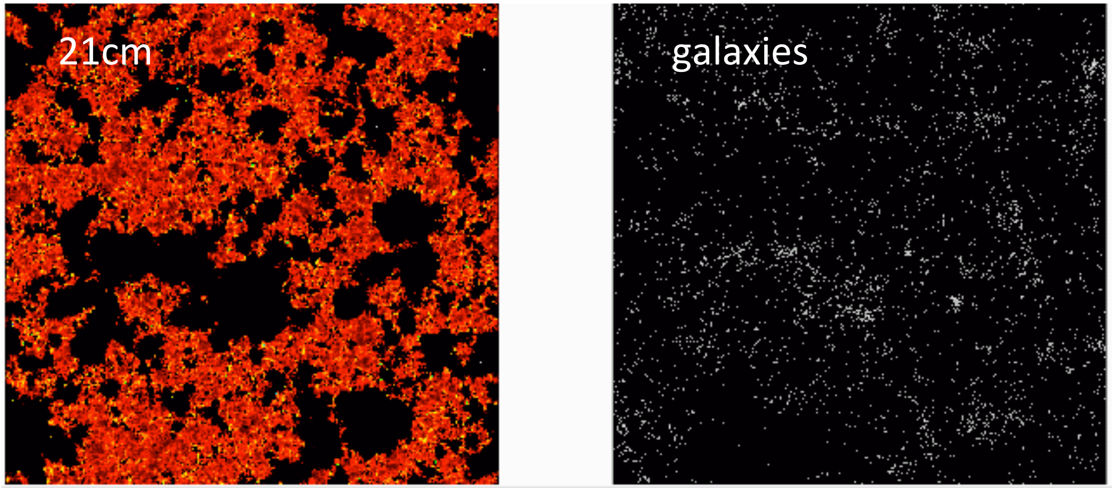

Lidz+ 2009

Cross-correlation 21cm-galaxy surveys

Wiersma+ 2013; Vrbanec+ in prep

3D spherically averaged cross power spectrum

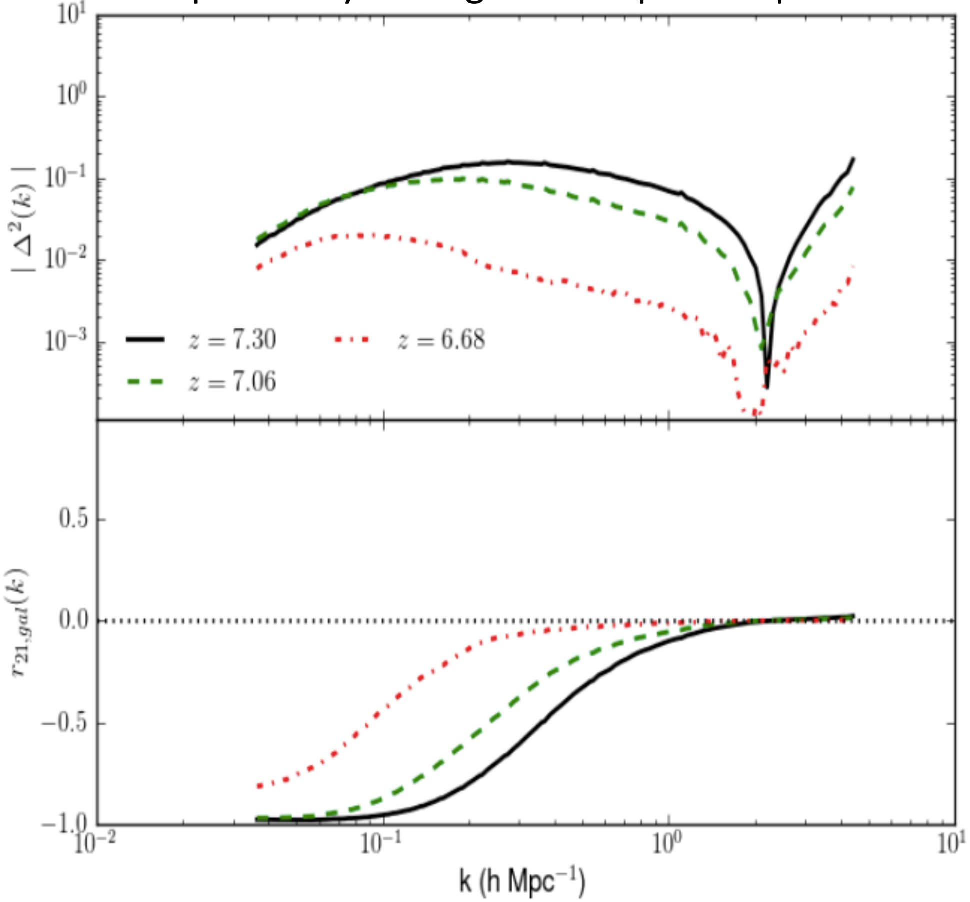

$$r_{21cm,gal}(k) = \frac{P_{21cm,gal}(k)}{\left[P_{21cm}(k)P_{gal}(k)\right]^{1/2}}$$

- ✧ Intensity of the power → volume average HI
- ✧ Correlation coefficient → typical dimension of the HII regions

Cross-correlation 21cm-galaxy surveys

Wiersma+ 2013; Vrbanec+ in prep

2D circularly averaged cross power spectrum

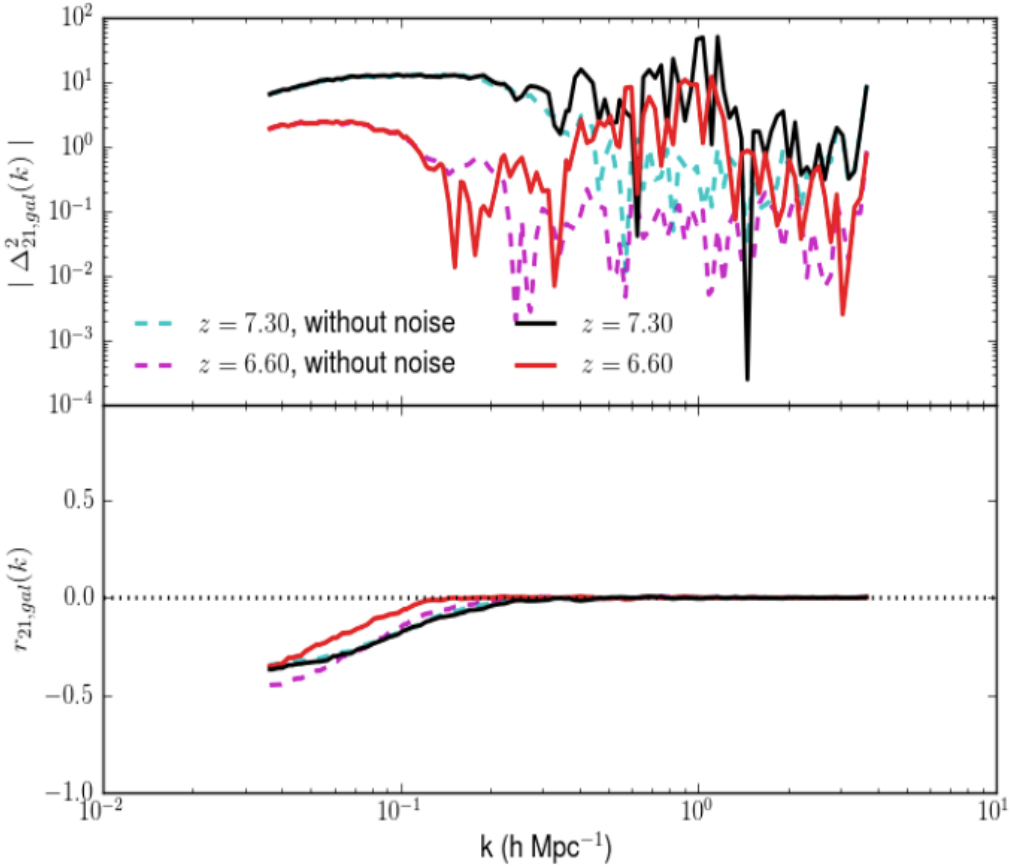

N(z=7.3)=125
N(z=6.6)=765

$$r_{21cm,gal}(k) = \frac{P_{21cm,gal}(k)}{\left[P_{21cm}(k)P_{gal}(k)\right]^{1/2}}$$

- ✧ Intensity of the power → volume average HI
- ✧ Correlation coefficient → typical dimension of the HII regions

Cross-correlation 21cm-galaxy surveys

Wiersma+ 2013; Vrbanec+ in prep

2D circularly averaged cross power spectrum

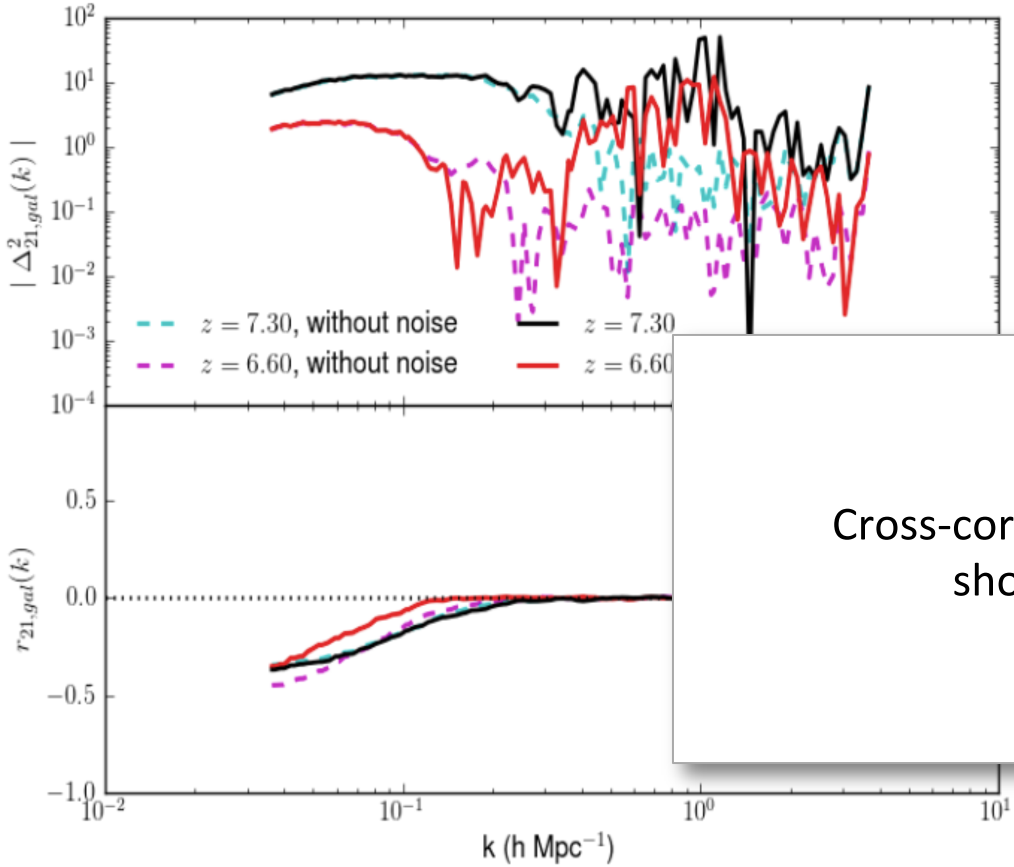

N(z=7.3)=125
N(z=6.6)=765

Cross-correlation LOFAR-SUBARU should be detectable

- ✧ Intensity of the power → volume average HI
- ✧ Correlation coefficient → typical dimension of the HII regions

REAL DATA!

Zaroubi+ in prep

NCP; HBA @ 115-170 MHz; 1 MHz resolution

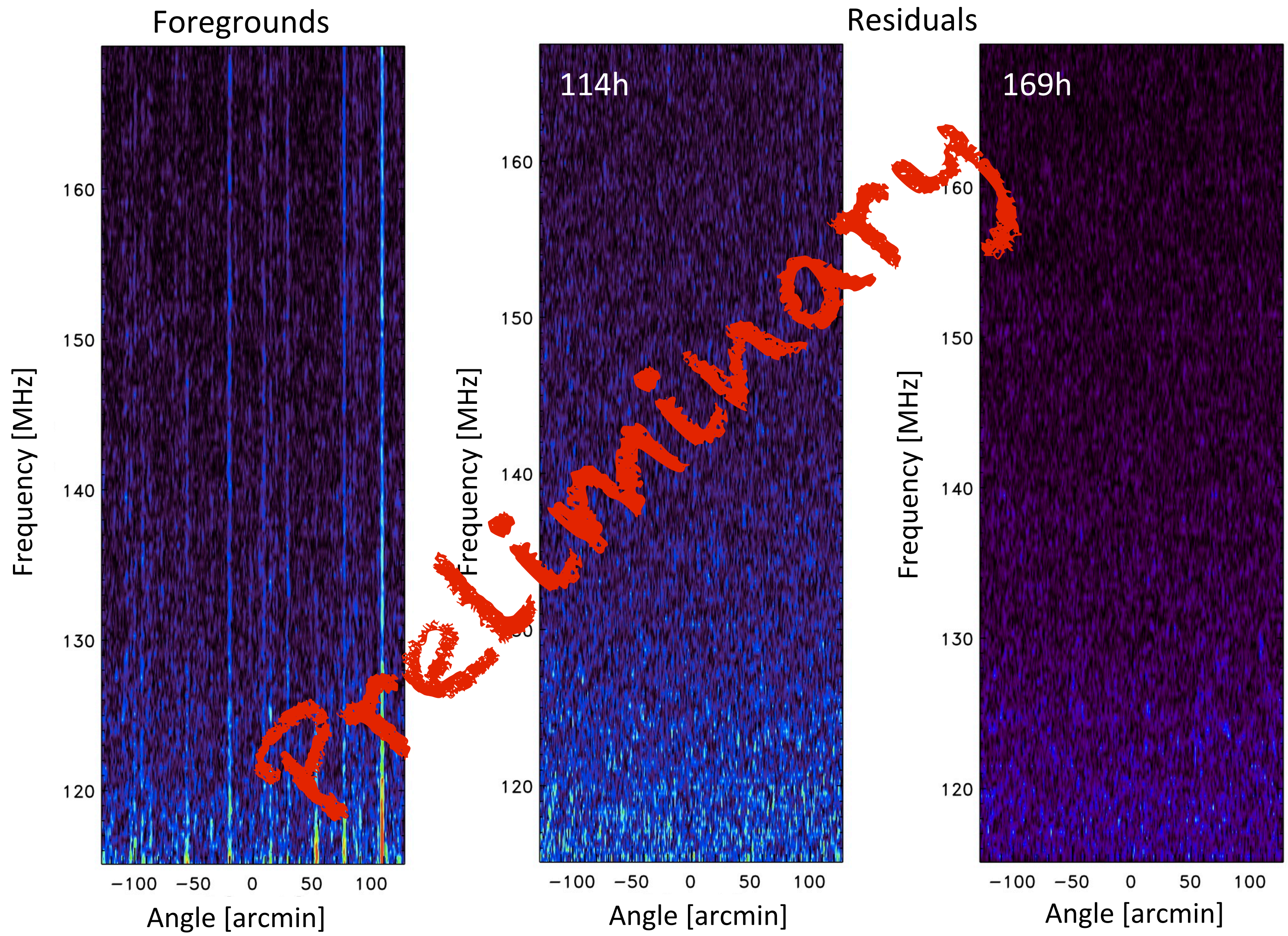

Conclusions

- ✧ LOFAR EoR project started in Dec 2012

- ✧ Cycle 0 (Dec2012 - Nov2013): 200h on 3C196 + 300h on NCP
  Cycle 1 (Nov2013 – May2014): 200h on 3C196 + 300h on NCP
  Cycle 2 (Summer 2014): 200h on NCP
  Cycle 3 (Nov2014 – May2015)

- ✧ We expect to obtain a statistical detection of the EoR, which will exclude some reionization scenarios and provide indirect constraints on high-z sources